R. & M. No. 3764

R. & M. No. 3764

PROCUREMENT EXECUTIVE, MINISTRY OF DEFENCE

AERONAUTICAL RESEARCH COUNCIL

REPORTS AND MEMORANDA

Non-linear Dynamic-Motion Characteristics of a Series of Missile Configurations from Simulated Flight Behaviour at Mach Numbers of 1·6 and 2·0

By I. M. TITCHENER

Aerodynamics Dept., R.A.E., Farnborough

LONDON: HER MAJESTY'S STATIONERY OFFICE

1975

PRICE £3·50 NET

Non-linear Dynamic-Motion Characteristics of a Series of Missile Configurations from Simulated Flight Behaviour at Mach Numbers of 1·6 and 2·0

By I. M. TITCHENER

Aerodynamics Dept., R.A.E., Farnborough

Reports and Memoranda No. 3764*
September, 1973

Summary

Non-linear oscillatory-motion histories, measured in the R.A.E. wind-tunnel/flight-dynamics simulator, are analysed. The resulting dynamic-motion characteristics for large-amplitude motions in the pitch plane are discussed in relation to the aerodynamic features of the various configurations tested, and a simple dimensionless mathematical model is specified.

* Replaces R.A.E. Technical Report 73145—A.R.C. 35 185

LIST OF CONTENTS

1. Introduction

An essential early step in the development of a projected guided-weapon system is the formulation of a reliable mathematical model to represent its dynamic-motion characteristics when responding to demands for acceleration normal to its flight path. This model is initially used to optimise the layout of the weapon and its control system and is subsequently incorporated in a comprehensive mathematical model for gaming studies.

To produce a mathematical model of the flight dynamics of a manoeuvring missile, the usual procedure is firstly to determine, either theoretically or by wind-tunnel testing, the aerodynamic force and moment functions over the range of possible flight conditions, and then to produce an adequate condensed mathematical representation of these non-linear functions. The dynamic response of the vehicle can then be computed by digital or analogue solution of its equations of motion, using the aerodynamic data as modelled. The computed dynamic response is in general significantly non-linear as a consequence of the form of the aerodynamic data and the equations of motion. This sequential approach to mathematical modelling is time-consuming and, with current trends towards more extreme angles of incidence during manoeuvres, resulting in strongly non-linear behaviour, is likely to become still more so.

As part of a fresh approach to these problems an integrated wind-tunnel/flight-dynamic simulator was developed[1,2] to provide directly the non-linear dynamic-response data for a manoeuvring flight vehicle without the intermediate stage of detailed analysis and mathematical modelling of the aerodynamic data.

Concurrently with the development of this facility theoretical work[3,4,5] yielded a technique for analysing the non-linear dynamic-response data which resulted in a particularly simple mathematical model of the dynamic-response characteristics.

Models of a series of related missile configurations representative of current trends in design[6] have been tested in the dynamic simulator to determine the damped free oscillatory response to a range of prescribed settings of the controls.[7–14] This Report analyses the measured data and discusses the resulting dynamic-motion characteristics in relation to the aerodynamic features of the various configurations.

In a further paper[15] the analysed dynamic-motion characteristics are combined with values of the steady-state-trim and control power, available from an associated series of wind-tunnel trim-boundary measurements.[7–14] These parameters can be expressed in an operational form relating the normal-acceleration response of the flight vehicle to the applied control displacement. Individual terms in these operator expressions have coefficients which themselves depend on the instantaneous amplitude of the response but the rates of change of the coefficients are small compared with the period and damping of the motion. These operational expressions constitute the desired concise mathematical model of the non-linear motion characteristics of the flight vehicle, and could be compounded with mathematical models of typical control elements for optimisation purposes or could be used subsequently in gaming studies.

2. Range of Model Configurations and Test Parameters

A set of nine different model configurations was tested, covering a range of wing and control-surface planforms. These configurations were intended to be broadly representative of current trends in the design of manoeuvrable missiles and the linear dimensions, mass and inertia of the vehicles simulated were selected accordingly. The nominal centre-of-gravity location for the tests was set by the criterion that adequate levels of normal acceleration should be produced for the available range of control-surface setting.

Layout sketches of the configurations are included in Figs. 1 and 2 and detailed dimensions are given in Ref. 6. Vehicle mass was 50 kg and the pitch inertia was 20 kg m^2. The angle of incidence of the vehicle could be simulated within the range $-0{\cdot}4 < \bar{w} < +0{\cdot}4$ for fixed control-surface settings up to ± 15 degrees.

Provision had been made in the construction of the wind-tunnel model for assembling the wings and control surfaces in a range of alternative fore-and-aft locations, to allow a detailed investigation of the influence of these parameters. In the event, the experimental programme was curtailed and only a preliminary assessment of the nine basic layouts could be completed. Layout 8, which had an annular wing, showed pronounced aerodynamic hysteresis effects with change in angle of incidence and was excluded from the dynamic-motion experiments.

The dynamic-simulation experiments were designed to yield information on the behaviour of the flight vehicle for free oscillation in the pitch plane, for each of a range of fixed settings of the control surfaces. Total velocity was constrained to remain uniform and simulations were carried out for flight at sea level at constant Mach numbers of 1·6 and 2·0. Initial conditions for a particular experiment were first established, consisting of the chosen control-surface setting and an angle of incidence which represents a large displacement from

the corresponding equilibrium (trimmed) incidence. The ensuing damped oscillatory motion was recorded for up to about one second of flight time. A second simulation was then carried out, for a slightly smaller initial displacement from the equilibrium angle of incidence, so giving an adequate indication of the variation in behaviour with change in local amplitude of oscillation.

It was planned, in the detailed analysis of the dynamic characteristics, to partition the total damping into two separate contributions suitable for recasting in non-dimensional form.* The necessary additional data were produced by repeating each simulation with the special condition of zero aerodynamic rate-damping (i.e. $C_{m_q} = 0$).

Independently of these dynamic simulation experiments detailed measurements were made of the static-aerodynamic characteristics of each configuration. Pitching-moment and normal-force data are summarised in Figs. 1 and 2 for each of the layouts now considered. These data cover the range of fixed control settings and relate to test Mach numbers of 1·6 and 2·0. Comprehensive aerodynamic data are reported in Refs. 7 to 14.

3. Online Monitoring of Dynamic Simulation Experiments and Offline Editing of Recorded Data

The progress of each experiment was observed qualitatively from the simulator control room, where the time-dependent parameters of the motion were displayed online using analogue X–Y plotting tables. This enabled the general operation of the simulator to be checked and runs repeated where necessary.

The trends of the resultant dynamic characteristics were monitored closely in the analysis laboratory using a specially developed analysis and display system[16] while the simulator tests were in progress. Results from this online analysis, comprising damping, frequency parameter and displacement of oscillation centre were displayed on a cathode-ray screen as functions of the local amplitude of oscillation. In this way any inconsistencies which might make repeat runs necessary, or any unexpected general trends making additional tests desirable, could be identified during the course of the test programme.

Detailed motion history data was recorded on magnetic tape in digital form. A stand-by paper-tape recording facility was also available within the online analysis system as a precaution in the event of a failure of the magnetic recorder; it was not found necessary to use this during the tests under consideration. A group of magnetic tapes was used, the recorded data being transcribed subsequently to punched cards for detailed analysis and at this stage a full line-printer record was produced. The tapes were then erased and used to record data during later experiments.

Preliminary editing of the recorded data was carried out during the transcription from magnetic tape to punched cards and some further hand editing of the punched cards was done as a result of a visual check of the line-printer record. The punched-card records were then in a satisfactory condition for detailed analysis using a general-purpose digital-computer program (Appendix A).

The computer analysis program included sub-routines which detected the majority of the remaining data errors, such cases were corrected manually and reprocessed. A small residue of data faults was detected

---

* It is shown in Ref. 5 that, for amplitudes of oscillation in the range from zero to 0·6, the total damping can be represented, with negligible error, by partitioning into two damping contributions arising from particular aerodynamic derivatives, thus

$$\lambda = \lambda_{(C_{m_q})} + \lambda_{(C_{z_{\dot{w}}})}.$$

It was also indicated that these damping contributions may be cast in non-dimensional forms

$$\left(2\tau\frac{i_B d}{V}\right)\lambda_{(C_{m_q})} \quad \text{and} \quad 2\tau\lambda_{(C_{z_{\dot{w}}})}$$

respectively. Partitioning of the frequency, ω^2 is unnecessary since, for the class of flight vehicle considered, the influence of $C_{z_{\dot{w}}}$ and C_{m_q} on frequency is negligible, thus

$$\omega^2 \simeq \omega^2_{(C_{m_{\dot{w}}})}.$$

Frequency may be expressed in the non-dimensional form $(\tau^2 i_B/-\mu)\omega^2$. Similarly the non-dimensional displacement of oscillation centre, δ/Θ is not affected by changes in $C_{z_{\dot{w}}}$ or C_{m_q}. The dynamic characteristics may thus be expressed in dimensionless forms based on

$$\lambda_{(C_{m_q})}, \qquad \lambda_{(C_{z_{\dot{w}}})}, \qquad \omega^2 \quad \text{and} \quad \delta/\Theta,$$

where $\lambda_{(C_{m_q})} = \lambda - \lambda_{(C_{z_{\dot{w}}})}$.

when the results of analysis were being assessed, these were corrected on an *ad hoc* basis and the data re-analysed.

A typical recorded motion history is shown in Fig. 3.

4. Analysis of Simulated Motion Histories

Records of computer analyses were produced as line-printer output headed by the serial number and initial conditions of the particular test, followed by the estimated equilibrium condition and set of values of time, peak angle of incidence, local amplitude of oscillation, damping, frequency parameter and normalised displacement of oscillation centre.

These data were first plotted individually for each test giving curves of damping, frequency parameter and oscillation centre each as a function of amplitude of oscillation. As an independent check the values of these parameters were estimated for the condition of small amplitude of oscillation using the relations given in Appendix B (equations (B-1), (B-2) and (B-3)), with aerodynamic data appropriate to the trimmed condition derived from the static-aerodynamic data previously recorded (Figs. 1 and 2, also Refs. 7 to 14). In general the degree of scatter shown in these results was satisfactory, a typical set of analysed results being given in Fig. 4.

The plotted results from individual analyses were next combined to define more closely the variation of the dynamic characteristics with change in the local amplitude of oscillation and to show their dependence on control setting. On theoretical considerations the difference between the frequency parameter, ω_0^2 and the frequency contribution, $\omega^2_{0(C_{m\bar{w}})}$ (*see* footnote, page 4) is relatively small for this class of flight vehicle.[5] In the corresponding case for finite amplitude the difference between ω^2 and $\omega^2_{(C_{m\bar{w}})}$ was found to be smaller than the scatter in these two sets of results over the range of amplitude investigated. The frequency parameter was therefore given approximately by the mean of ω^2 and $\omega^2_{(C_{m\bar{w}})}$ (Fig. 5). If desired, a small correction may be estimated to show the effect of the contribution $\omega^2_{0(C_{m_q}, C_{z\bar{w}})}$ on the results for small amplitude, using the relation given in Appendix B (equation (B-4)) with appropriate data from the results for damping, λ_0 and damping contribution, $\lambda_{0(C_{z\bar{w}})}$.

The normalised displacement of oscillation centre was not affected by the condition ($C_{m_q} = 0$) and the two sets of results for this parameter were therefore combined (Fig. 6).

Sets of plotted results, comprising damping λ, damping contribution $\lambda_{(C_{z\bar{w}})}$, frequency parameter ω^2 and displacement of oscillation centre δ/Θ, are presented in Figs. 9 to 25, for test Mach numbers of 1·6 and 2·0.

5. Trends of Dynamic Characteristics Related to Static-Aerodynamic Data

5.1. Classification of Static-Aerodynamic Data

The relation between the measured static-aerodynamic data and the analysed dynamic characteristics is now considered. The general form of the normal-force data, C_z is the same for all configurations tested, having a negative gradient becoming larger with increasing angle of incidence. The magnitude of normal force, and consequently also of the derivative $C_{z\bar{w}}$, varies among the configurations tested by about 50 per cent for a given angle of incidence, $\bar{w}$.

The pitching moment due to angle of incidence may assume two distinct non-linear forms. In some cases (e.g. group A comprising configurations 1, 2R, 3, 4, 6 and 7) the pitching moment has a negative gradient becoming numerically larger with increasing angle of incidence. In other cases (e.g. group B comprising configurations 2F, 5 and 9) the gradient for small angle of incidence is positive, representing a local instability, stability is regained for moderate values of $\bar{w}$, the gradient again becoming progressively more negative. These two distinct forms of pitching-moment characteristic give rise to different dynamic behaviour, chiefly affecting the frequency parameter and the displacement of oscillation centre. This has been considered theoretically for an idealised flight vehicle,[5] for a normal-force characteristic similar to the general form of the present data. Some general results of this theoretical work are summarised in Appendix C.

5.2. Influence of Static-Aerodynamic Data on Dynamic-Response Characteristics

For those configurations having monotonic pitching-moment curves ('form 3' of Ref. 5) the theoretical analysis indicated a strong increase in damping with increase of control setting, for small-amplitude motions, with relatively small changes from these values for motions of large amplitude. Similar results are obtained

from analysis of the simulated motion histories for group A. In some cases the variation of damping with control setting is more non-linear than indicated theoretically as a consequence of the detailed form of the derivative $C_{z_{\bar{w}}}$ and of the non-linear variation in control effectiveness, which was taken to be linear in the theoretical work.

For the configurations having a local instability ('form 6' of Ref. 5) theoretical analysis indicated more pronounced changes in damping with change in amplitude. Again similar trends are shown in the analysis of simulator data of group B.

The frequency parameter, for pitching-moment characteristics similar to those of 'form 3' (i.e. a 'hard' system, *see* Appendix C), was indicated theoretically to increase strongly with increase in control setting, for small-amplitude motions, and to change appreciably from these values for motions of large amplitude. The results of simulation tests for configurations in group A show similar trends again with further variation arising from the detailed form of the derivative $C_{m_{\bar{w}}}$ and from non-linearity of control effectiveness. It is noted that in almost every instance the change in frequency parameter with amplitude and the trend in damping with amplitude are consistently of opposing senses, as was indicated by the theoretical work.

For configurations having a local instability (form '6') theoretical analysis indicated more pronounced changes in frequency parameter with change in both control setting and in amplitude. These detailed trends are confirmed by the analysed results of the simulator data for group B.

The normalised displacement of oscillation centre, δ/Θ, was shown theoretically to be strongly dependent on the form of the pitching-moment characteristic. For 'hard' pitching-moment characteristics ('form 3') the gradient of δ/Θ with amplitude was zero for zero control setting, increasing at first rapidly with control setting and decreasing slightly for the largest control setting. For the pitching moment with local instability ('form 6') the gradient of δ/Θ with amplitude was large for zero control setting, decreasing progressively with increase in control setting. The above applies to motions of small amplitude, as larger amplitudes are considered so the gradient of δ/Θ tends to decrease, eventually reaching a peak of δ/Θ and thereafter becoming negative. This non-linearity in δ/Θ extends to smaller amplitudes in the case of small control settings than in the case of large settings, for both 'form 3' and 'form 6'. In the latter example the degree of the non-linearity is more extreme.

The results of simulation tests for group A show trends of oscillation control similar to those derived theoretically for 'form 3', with some small reservations concerning the results for configurations 6 and 7, where the results for the largest control setting are non-linear over a wider range of amplitude than expected. For group B the trends are as indicated theoretically for 'form 6', the progression from the mildly non-linear pitching-moment characteristics of configuration 8 through configuration 5 to the highly non-linear pitching moments of configuration 2F being accompanied by increasingly extreme changes in δ/Θ.

6. Discussion

At the preliminary stage of analysis of each response history an estimate is made of the equilibrium condition, $\bar{w}_T$, based on the weighted mean of the last three fitted peaks of the data record (equation (A-3) and Fig. 3). In some cases this estimate is slightly in error, as a result of scatter in the data. Since the amplitude of oscillation in this region is small, the effect of a small error in $\bar{w}_T$ is to give relatively large local errors in the analysed displacement of oscillation, δ, while the values of δ for the early part of the record, where amplitude is larger, are not significantly affected. This could be resolved by correcting the estimate of $\bar{w}_T$ using an independent value based on the static aerodynamic data and repeating the analysis for displacement, δ. In practice the original analysis yielding normalised displacement, δ/Θ as a function of amplitude, Θ was corrected satisfactorily by neglecting the analysed results for small amplitude and fitting to the values for large amplitude, the fitted curve being extended to intersect the origin. This procedure is illustrated in Fig. 6 and is confirmed by an independent estimate for small amplitude based on equation (B-3). The effect of a small error in $\bar{w}_T$ on the analysis of damping and frequency parameter is negligible.

It is noted that the scatter in the analysed values of oscillation centre for zero control setting (for example Fig. 6) is generally slightly greater than for the other control settings. This is attributed to random small errors in rigging the control surfaces of the model, which would give rise to asymmetric behaviour. Similar small rigging errors may have affected also the particular data for a control setting of 15 degrees shown in Fig. 6. In this case the empirical result for small amplitude, based on equation (B-3), is in poor agreement with the analysed data, in contrast to the excellent agreement generally obtained.

Analysed dynamic characteristics are presented in carpet form to improve confidence in those areas where the data was relatively sparse, such as the extreme of the large amplitude region.

In studies of aerodynamic characteristics the conventional practice is to express such results as functions of the trimmed angle of incidence, $\bar{w}_T$. However it is intended to embody the results of the present investigation, which examined the open-loop dynamic behaviour of the flight vehicle, in a mathematical model of its dynamic characteristics for subsequent applications such as studies of control systems. In this context a more appropriate form of presentation is in terms of the control setting, η, since this is the input applied to the system.

The centre-of-gravity position for each configuration tested was specified using the criterion that a given order of trimmed normal force should result for the maximum available setting of the control. It was originally intended that the next stage in the experimental survey would be an investigation of the influence of alternative positions of the centre of gravity on the dynamic characteristics for motions of large amplitude. Using the recorded static-aerodynamic data available from the present tests the dynamic characteristics for alternative positions of centre of gravity can be assessed very simply for the restricted case of oscillations of small amplitude.

The static-aerodynamic data indicates non-linear trends in control effectiveness for large control settings, these are adequately covered by the intervals in control setting specified for the tests. Certain local non-linearities in control effectiveness are also indicated for small control settings which may be equally significant in their effect on the dynamic behaviour. For example in the case of configuration 2F (Fig. 1) for zero angle of incidence, $\bar{w}$, the incremental pitching moment, C_m arising from control setting, η is less over the interval $\eta = 0$ degrees to $\eta = 5$ degrees than for the interval $\eta = 5$ degrees to $\eta = 10$ degrees. Data showing the resultant dynamic characteristics for control settings of 0, $2\frac{1}{2}$ and 5 degrees is included in Figs. 11 and 12, this indicates local changes in behaviour for the $2\frac{1}{2}$ degree setting significantly differing in form from that for neighbouring settings. Similar trends in the static-aerodynamic data for small control settings are present for several of the other configurations, the corresponding dynamic behaviour for large-amplitude motions was not available for analysis. It is suggested that these particular non-linearities in control effectiveness may be a consequence of the location of the control surfaces within the wake of the wings for small control setting and for small angles of incidence of the vehicle.

It has been shown in Section 5 that the trends of the dynamic characteristics are related to the salient features of the static-aerodynamic data. In passing it is worthy of note that the damping contribution, $\lambda_{(C_{m_q})}$ arising from the aerodynamic rate-moment, $M(q)$ constitutes, for several of the configurations examined, a relatively minor part of the damping, λ, in some cases representing as little as 20 per cent of the total damping and in no instance exceeding 50 per cent. The derivative C_{m_q} is normally either estimated theoretically or determined from dynamically-scaled tests in a wind tunnel. It has been shown[5] that the damping contribution, $\lambda_{(C_{m_q})}$ may be taken to be directly proportional to the derivative C_{m_q}. Thus the damping contribution, $\lambda_{(C_{m_q})}$ appropriate to an alternative value of the derivative may be estimated directly and combined with the damping contribution, $\lambda_{(C_{z_{\bar{w}}})}$ already determined to give the damping, λ for the revised estimate of C_{m_q}.

A technique was developed in Ref. 5 for the mathematical modelling of the dynamic response characteristics which involved partitioning the damping, λ over the range of amplitude to give damping contributions $\lambda_{(C_{z_{\bar{w}}})}$ and $\lambda_{(C_{m_q})}$. These parameters, together with the frequency parameter, ω^2 and the displacement of oscillation centre, δ would be expressed in dimensionless form to give general results applicable to other vehicles of the same geometric shape and operating at the same Mach number. The appropriate dimensionless groups and relations are given in Appendix D. The reported dynamic-simulation tests were planned for a common set of vehicle parameters and operating conditions, for each of the configurations tested. Thus direct comparisons may be made between results for the various configurations as presented. The damping parameters have been left in the forms λ and $\lambda_{(C_{z_{\bar{w}}})}$; if it should be desired to convert these results to dimensionless form for application to other flight conditions or combinations of vehicle parameters then $\lambda_{(C_{m_q})}$ must first be deduced using equation (D-1). For illustration the results for configuration 7, Mach numbers 1·6 to 2·0, are fully partitioned and presented in Fig. 26, while the appropriate parameters to be used in the final stage of the analysis to give dimensionless forms are tabulated in Appendix D.

The analysed results show that the dependence on amplitude of each of the dynamic-motion parameters is in general of the same order as its dependence on control setting over the range of amplitude, Θ and control setting, η investigated. A convenient mathematical model for the dynamic characteristics of any particular configuration may therefore be constructed by expressing each parameter as a low-order polynomial function in terms of both Θ and η. In this model δ/Θ and the dimensionless expressions for $\lambda_{(C_{z_{\bar{w}}})}$, $\lambda_{(C_{m_q})}$ and ω^2 ((D-3), (D-4) and (D-5)) would be represented in a compact form.

The relation of the dynamic characteristics to the geometric layout of the vehicle configuration, and the presentation of the mathematical model in operator form, are the subject of a further report, to be published.[15]

7. Conclusions

Experimental data from simulation studies of a series of weapon configurations have been analysed. Non-linear dynamic characteristics for Mach numbers of 1·6 and 2·0 are presented for large-amplitude motions in the pitch plane.

The various configurations tested have been broadly classified on the basis of their static-stability characteristics, enabling their measured dynamic behaviour to be compared with that previously calculated for a number of idealised cases.

In general the frequency for small amplitudes of oscillation increased with larger control setting, reflecting the increasing stiffness of the configurations with angle of incidence. The variation of frequency with amplitude of oscillation depended on the control setting. At zero control setting the frequency increased with amplitude, while at the larger control settings the opposite occurred. At moderate amplitudes there were in some cases pronounced changes in frequency, particularly for small control settings corresponding to the greatest local non-linearity in the pitching-moment curves.

Changes in damping with amplitude and control setting were primarily a function of the effective normal-force derivative, which was determined by the corresponding trim angle of incidence. For small amplitude the damping increased at the larger values of control setting, though generally in a more linear manner than was the case for the frequency. Variation of damping with amplitude, for a given control setting, was generally more pronounced for the larger control settings.

Normalised displacement of the oscillation centre showed a wide range of behaviour among the configurations examined, being particularly sensitive to local changes in the aerodynamic characteristics. The significant criterion for its general behaviour was the occurrence of aerodynamic instability. Those configurations having a local instability (2F, 5 and 9) had progressively larger initial gradients of oscillation centre with respect to amplitude for smaller control settings. In the case of configurations having stabilising aerodynamic characteristics the same trend occurred for large control settings, although the actual values of displacement were generally diminished. In this case there was no displacement of centre of oscillation for zero control setting. For larger amplitudes of oscillation the normalised displacement of oscillation centre was in all cases appreciably reduced below the values corresponding to the gradient for small amplitude.

Earlier theoretical work had shown that the dynamic-motion parameters depended on both amplitude and control setting and that these two variables were of approximately equal significance. The trends of the reported analysis confirmed this result for the ranges of amplitude and control setting examined.

A simple dimensionless mathematical model of the dynamic characteristics was specified, which was applicable to any particular vehicle configuration, based on low-order polynomial series expansions in terms of both local amplitude and control setting.

Significant local non-linearities in control effectiveness, for small control settings, were identified in the case of certain configurations but this aspect was not investigated in detail since the planned experimental programme was curtailed. A simple analysis has been indicated which will enable trends of the intended experiments on displacement of centre of gravity to be estimated using data recorded during the completed part of the investigation.

8. Further Work

The scope of the present investigation was restricted. It has shown that assessments over a range of small control settings are desirable to give a proper estimate of the non-linear behaviour in this region of practical importance. This could be done by digital-computer analysis if static-aerodynamic data were first obtained by a series of short conventional wind-tunnel tests.

The experimental programme as originally planned included further investigations of the non-linear dynamic characteristics for a range of positions of the centre of gravity and, by appropriate adjustments of wing and control-surface location, the optimisation of the layout of each of the basic configurations.

LIST OF SYMBOLS

B	Moment of inertia about G_y
C_m	$= \dfrac{M(\bar{w}, \eta)}{\frac{1}{2}\rho V^2 S d}$
C_{m_q}	Aerodynamic/pitch-damping derivative
$C_{m_{\bar{w}}}$	$= \dfrac{\partial C_m}{\partial \bar{w}}$
C_z	$= \dfrac{Z(\bar{w}, \eta)}{\frac{1}{2}\rho V^2 S}$
$C_{z_{\bar{w}}}$	$= \dfrac{\partial C_z}{\partial \bar{w}}$
G_x, G_y, G_z	Principal body axes
M_q	$= \dfrac{\partial M}{\partial q}$
$M(\bar{w})$	Aerodynamic moment about axis G_y
$M_{\bar{w}}$	$= \dfrac{\partial M}{\partial \bar{w}}$
S	Reference area $\left(= \dfrac{\pi}{4} d^2\right)$
V	Flight velocity $(= (u^2 + w^2)^{\frac{1}{2}})$
$Z(\bar{w})$	Aerodynamic force along axis G_z
$Z_{\bar{w}}$	$= \dfrac{\partial Z}{\partial \bar{w}}$
d	Body maximum diameter (reference length)
i_B	Inertia coefficient about G_y $\left(= \dfrac{B}{md^2}\right)$
m	Mass of vehicle
q	Angular velocity, relative to earth axes, about axis G_y
t	Time
τ	Unit of aerodynamic time $\left(= \dfrac{m}{\frac{1}{2}\rho V S}\right)$
u	Translational-velocity component along axis G_x
w	Translational-velocity component along axis G_y
$\bar{w}$	$= \dfrac{w}{V}$
$\bar{w}_T$	Value of dependent variable at equilibrium (trim)
Θ	Amplitude
δ	Displacement of local centre of oscillation
η	Control-surface setting (degrees)
λ	Damping $(= \dot{\Theta}/\Theta)$
μ	Flight-vehicle relative density $\left(= \dfrac{m}{\frac{1}{2}\rho S d}\right)$
ρ	Atmospheric density
ω	Fundamental frequency

Subscripts

T	Equilibrium (trimmed) condition about reference centre of gravity
i	Initial value
0	Small amplitude about the trimmed condition
(C_{m_q})	Contribution arising from C_{m_q}
$(C_{z_{\bar{w}}})$	Contribution arising from $C_{z_{\bar{w}}}$
$(C_{m_q}, C_{z_{\bar{w}}})$	Contribution arising from C_{m_q} and $C_{z_{\bar{w}}}$

Note

For convenience the following shortened expressions are adopted, having the meanings attached to the symbols:

Angle of incidence, $\bar{w}\left(=\frac{w}{V}\right)$

Frequency parameter, ω^2

Oscillation centre (i.e. normalised displacement of local centre of oscillation), δ/Θ.

REFERENCES

No.	Author(s)	Title, etc.
1	L. J. Beecham, W. L. Walters and D. W. Partridge	Proposals for an integrated wind tunnel flight-dynamics simulator system. A.R.C. C.P. 789 (1962).
2	I. M. Titchener and B. E. Pecover . .	An integrated facility for the simulation of some non-linear flight dynamic problems. R.A.E. Technical Memorandum Aero 1324 A.R.C. 33240 (1971).
3	L. J. Beecham and I. M. Titchener . .	Some notes on an approximate solution for the free oscillation characteristics of non-linear systems typified by $\ddot{x} + F(x, \dot{x}) = 0$. A.R.C. R. & M. 3651 (1969).
4	I. M. Titchener	Development of a technique for the analysis of non-linear dynamic characteristics of a flight vehicle. R.A.E. Technical Report 73023 A.R.C. 34708 (1973).
5	I. M. Titchener	The analysis and mathematical modelling of non-linear characteristics of large-amplitude motions of flight vehicles. R.A.E. Technical Report to be published.
6	B. E. Pecover	Some weapons configurations to be tested in the R.A.E. wind tunnel/flight dynamics simulator in aid of mathematical modelling. R.A.E. Technical Memorandum Aero 1358 A.R.C. 33373 (1971).
7	B. E. Pecover and V. G. Quincey . .	Stability and control measurements on one of a series of weapon configurations using the R.A.E. wind tunnel/flight dynamics simulator—configuration 1. R.A.E. Technical Memorandum Aero 1518 A.R.C. 34979 (1973).
8	V. G. Quincey, J. F. G. Warren and B. E. Pecover	Stability and control measurements on one of a series of weapon configurations using the R.A.E. wind tunnel/flight dynamics simulator—configuration 9. R.A.E. Technical Memorandum Aero 1515 A.R.C. 35226 (1973).
9	B. E. Pecover and Patricia M. Willatts	Stability and control measurements on one of a series of weapon configurations using the R.A.E. wind tunnel/flight dynamics simulator—configuration 4. R.A.E. Technical Memorandum Aero 1517 A.R.C. 34934 (1973).
10	J. F. G. Warren and V. G. Quincey	Stability and control measurements on one of a series of weapon configurations using the R.A.E. wind tunnel/flight dynamics simulator—configuration 3. R.A.E. Technical Memorandum Aero 1516 A.R.C. 35052 (1973).
11	B. E. Pecover, Patricia M. Willatts and H. Purvis	Stability and control measurements on one of a series of weapon configurations using the R.A.E. wind tunnel/flight dynamics simulator—configuration 2. R.A.E. Technical Memorandum Aero 1593 (1974).
12	J. F. G. Warren and V. G. Quincey	Stability and control measurements on one of a series of weapon configurations using the R.A.E. wind tunnel/flight dynamics simulator—configuration 5. R.A.E. Technical Memorandum Aero 1561 A.R.C. 35709 (1974).

No.	Author	Title, etc.
13	B. E. Pecover and Patricia M. Willatts	Stability and control measurements on one of a series of weapon configurations using the R.A.E. wind tunnel/flight dynamics simulator—configuration 6. R.A.E. Technical Memorandum Aero 1551 A.R.C. 35216 (1973).
14	B. E. Pecover and Patricia M. Willatts	Stability and control measurements on one of a series of weapon configurations using the R.A.E. wind tunnel/flight dynamics simulator—configuration 7. R.A.E. Technical Memorandum Aero 1560 (1974).
15	I. M. Titchener	(R.A.E. Technical Report, to be published).
16	R. P. Purkiss and N. J. Benger . .	An on-line analyser using visual techniques for processing of non-linear dynamic response data. R.A.E. Technical Report 73075 (1973).
17	H. H. B. M. Thomas and S. Neumark	Interim Note on stability and response characteristics of supersonic aircraft (linear theory). R.A.E. Technical Note Aero 2412 A.R.C. 18263 (1955).

APPENDIX A

Digital-Computer Program for Analysis of Non-linear Dynamic-Response Data

In Ref. 4 a simple technique is described for analysing a given non-linear response history. This gives an expression for damping,

$$\lambda_{(\Theta=\Theta_2)} \simeq \frac{\Delta_2^2 \ln(\Theta_3/\Theta_2) + (\Delta_3 - \Delta_2)^2 \ln(\Theta_2/\Theta_1)}{\Delta_2\Delta_3(\Delta_3 - \Delta_2)} \tag{A-1}$$

where Θ_n is the amplitude of the envelope at the peak of the nth half cycle, t_n is the elapsed time to Θ_n and $\Delta_n = t_n - t_{\text{REF}}$. The frequency parameter, ω^2 is given by

$$\omega^2_{(\Theta=\Theta_2)} = \left(\frac{2\pi}{\Delta_3}\right)^2 \tag{A-2}$$

and the displacement of the centre of oscillation, δ is estimated by constructing the mean of the envelopes of peaks (Fig. 3) and deducing the displacement from the trim angle of incidence, $\bar{w}_T$.

The computer program incorporates the above analysis, the local peaks of the response history being first determined by individual local least-squares fitting and the trim angle of incidence, $\bar{w}_T$, being estimated from the weighted mean of the last-three peaks of the response history,

$$\bar{w}_T = \frac{\hat{\bar{w}}_{(N-2)} + 2\hat{\bar{w}}_{(N-1)} + \hat{\bar{w}}_N}{4} \tag{A-3}$$

where $\hat{\bar{w}}_N$ is the normalised translational-velocity component for the last peak. Steps in the analysis of a typical motion history are shown in Figs. 3 and 4.

APPENDIX B

General Expressions for Dynamic Characteristics for Motions of Small Amplitude

Standard linear theory[17] gives damping,

$$\lambda_0 = \frac{1}{2}\left(\frac{M_q}{B} + \frac{(Z_{\bar{w}})_T}{mV}\right) \tag{B-1}$$

and frequency parameter,

$$\omega_0^2 = -\frac{(M_{\bar{w}})_T}{B} + \frac{M_q}{B}\frac{(Z_{\bar{w}})_T}{mV}. \tag{B-2}$$

An empirical form for normalised displacement of centre of oscillation, δ/Θ is given in Ref. 5:

$$-(\delta/\Theta)_0 = -\frac{1}{6}\frac{(\partial^2 C_m/\partial \bar{w}^2)_T}{(\partial C_m/\partial \bar{w})_T}\Theta. \tag{B-3}$$

The relatively small second term in the expression for frequency parameter (equation (B-2)) may be estimated alternatively from the damping, λ_0 and damping contribution, $\lambda_{0(C_{z\bar{w}})}$:

$$\omega_0^2 - \omega_{0(C_{m\bar{w}})}^2 = \frac{M_q}{B}\frac{(Z_{\bar{w}})_T}{mV}$$
$$= 2\lambda_{0(C_{mq})} 2\lambda_{0(C_{z\bar{w}})},$$

i.e.

$$\omega_0^2 - \omega_{0(C_{m\bar{w}})}^2 = 4\{\lambda_0 - \lambda_{0(C_{z\bar{w}})}\}\lambda_{0(C_{z\bar{w}})}. \tag{B-4}$$

APPENDIX C

Theoretical Forms of Dynamic Characteristics for Non-linear Motions of Large Amplitude of an Idealised Flight Vehicle

An earlier theoretical analysis[5] surveyed the nature of the dynamic-response characteristics which would result for a range of assumed aerodynamic normal-force and pitching-moment functions of an idealised flight vehicle.

The aerodynamic normal force assumed throughout the theoretical analysis had a negative gradient for small angle of incidence, $\bar{w}$, the gradient becoming numerically greater with increasing angle of incidence.

The aerodynamic pitching-moment forms arising in the simulator investigation correspond generally with two of the assumed forms of the theoretical work, a 'hard' form for which the gradient of pitching moment with angle of incidence, $C_{m_{\bar{w}}}$ was negative for small angle of incidence, $\bar{w}$ and increasingly so for large $\bar{w}$; and a modified 'hard' form showing a local destabilising change of sign of $C_{m_{\bar{w}}}$ for small angle of incidence. The term 'hard' is commonly used in this context by analogy with the case of an oscillating spring-mass system where the spring has a steepening force/extension characteristic. Conversely a 'soft' spring in that example would have a diminishing gradient of restoring force.

The results of the theoretical survey for these two aerodynamic forms are reproduced in Figs. 7 and 8 to indicate qualitative trends which may be anticipated in the present analysis. The comparison with trends of the simulator results is made in Section 5.2.

APPENDIX D

Dimensionless Expressions for Dynamic Characteristics

In Ref. 5 it was shown that the damping, λ could be partitioned, yielding a relation convenient in analysis of motions of large amplitude

$$\lambda = \lambda_{(C_{z_{\bar{w}}})} + \lambda_{(C_{m_q})}. \tag{D-1}$$

It was also shown that, to a good approximation, the frequency parameter, ω^2 was given by

$$\omega^2 \simeq \omega^2_{(C_{m_{\bar{w}}})}. \tag{D-2}$$

Dimensionless expressions were proposed for these parameters, based on their theoretical forms for motions of small amplitude. Thus damping with the condition ($C_{m_q} = 0$) may be represented by the expression

$$2\tau\lambda_{(C_{z_{\bar{w}}})} \tag{D-3}$$

and damping with the condition ($C_{z_{\bar{w}}} = 0$) may be represented by the expression

$$2\tau\frac{i_B d}{V}\lambda_{(C_{m_q})}. \tag{D-4}$$

The frequency parameter, ω^2 is represented in the expression

$$\frac{\tau^2 i_B}{-\mu}\omega^2 \tag{D-5}$$

and the displacement of oscillation centre, δ is represented in dimensionless form, normalised with respect to amplitude

$$\frac{\delta}{\Theta}.$$

The following values were used in the simulations for each of the configurations tested:

vehicle mass,	$m = 50$ kg
moment of inertia,	$B = 20$ kg m^2
body maximum diameter,	$d = 0{\cdot}2\ m$
reference area,	$S = 0{\cdot}03142\ m^2$
atmospheric density,	$\rho = 1{\cdot}225$ kg m^{-3}
flight velocity,	$V = 544{\cdot}7$ ms^{-1} (for $M = 1{\cdot}6$)
	$= 680{\cdot}9$ ms^{-1} (for $M = 2{\cdot}0$)

The groups specified in the dimensionless expressions (D-3), (D-4), (D-5) result:

Group	$M = 1{\cdot}6$	$M = 2{\cdot}0$
2τ	9·54	7·63
$2\tau\frac{i_B d}{V}$	0·0350	0·0224
$\tau^2\frac{i_B}{-\mu}$	−0·01751	−0·01121

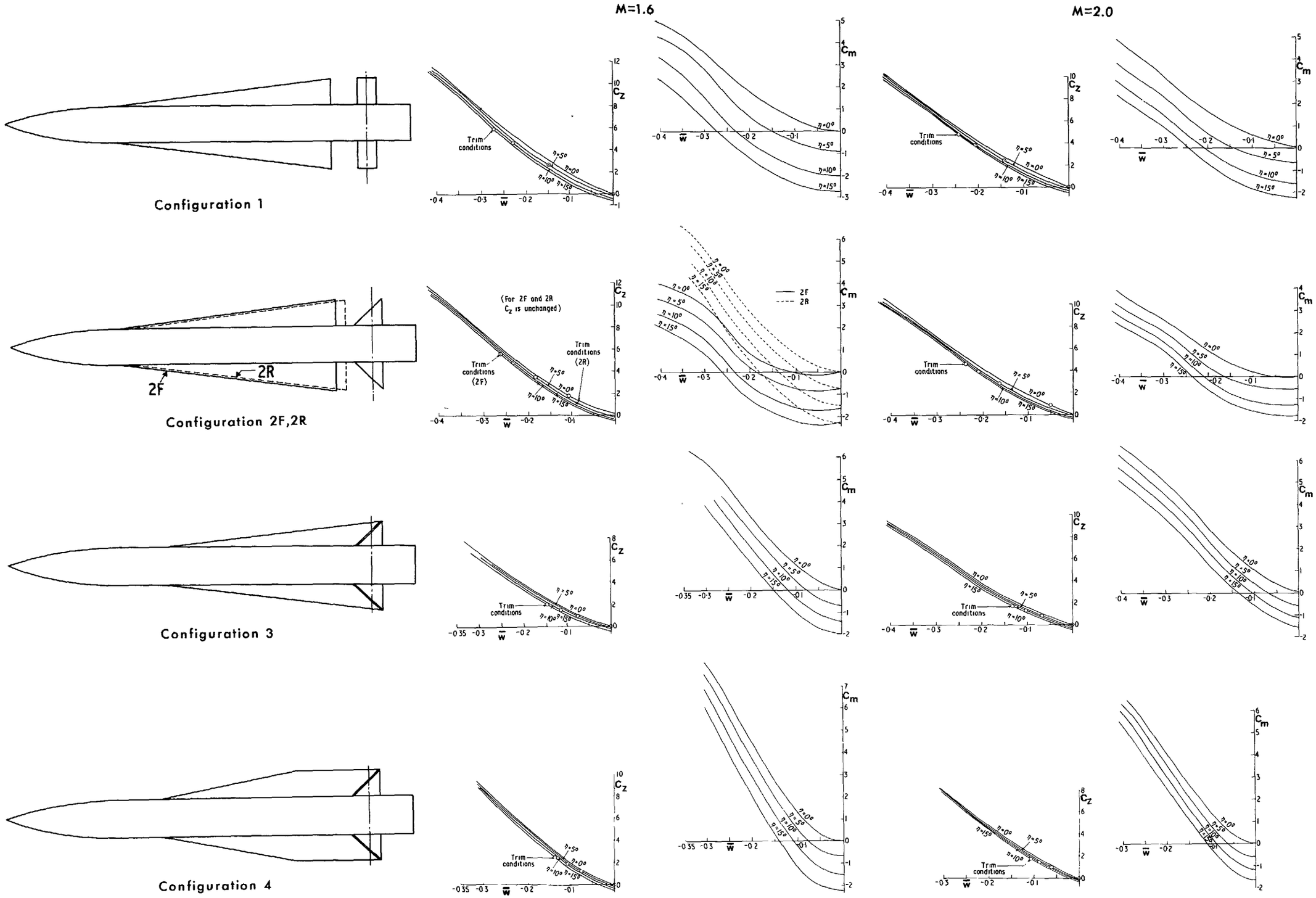

FIG. 1. Layouts of configurations 1–4 and static aerodynamic data.

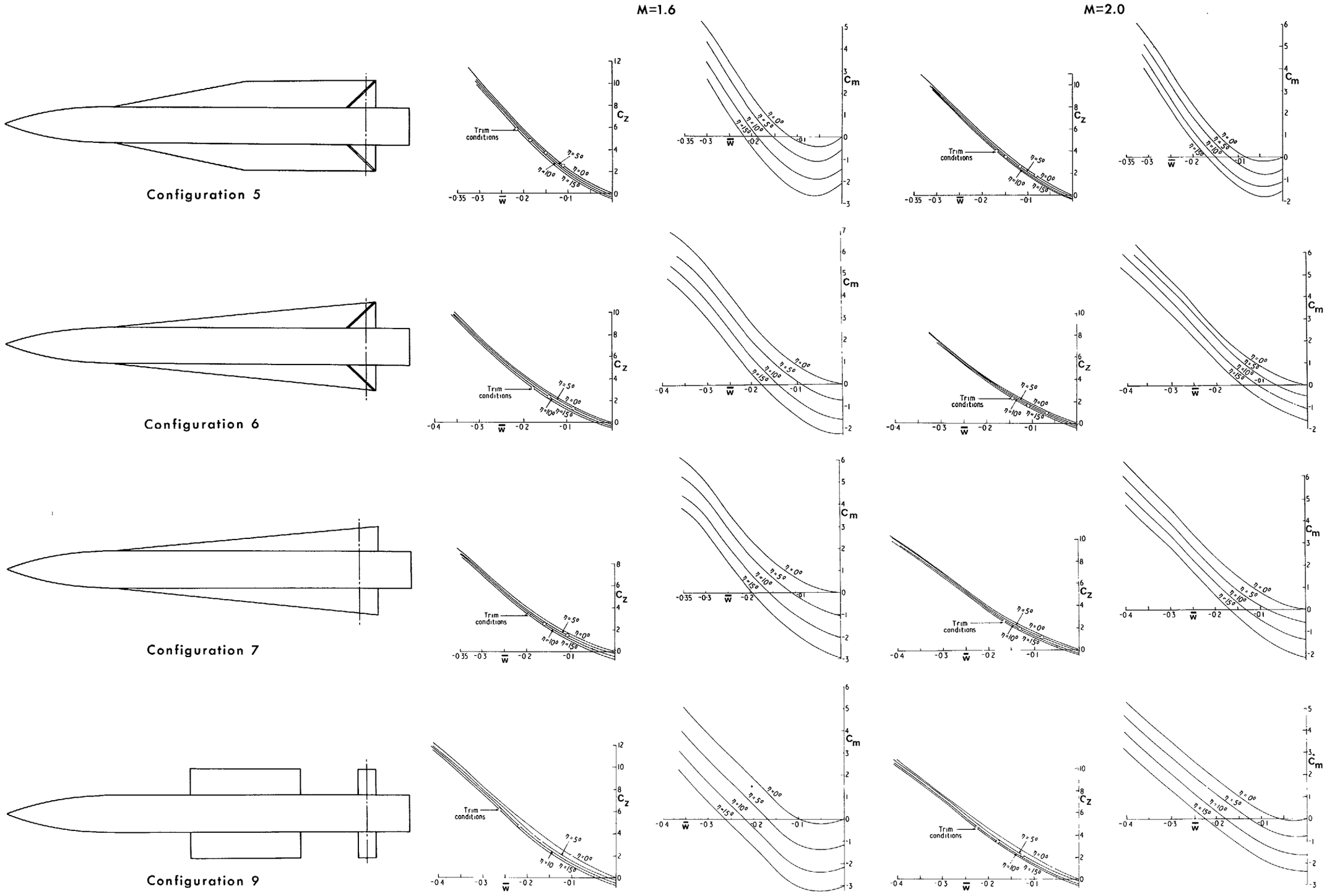

FIG. 2. Layouts of configurations 5–7, 9 and static aerodynamic data.

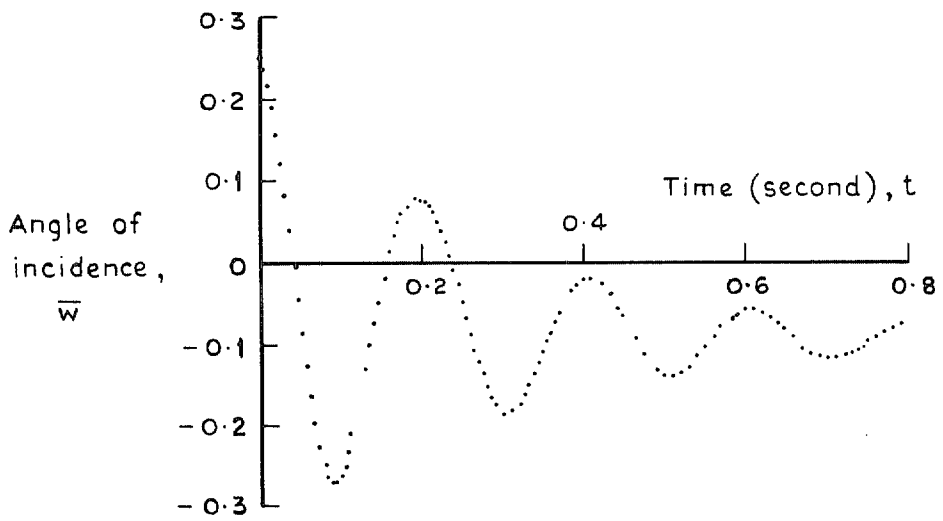

Recorded data after editing

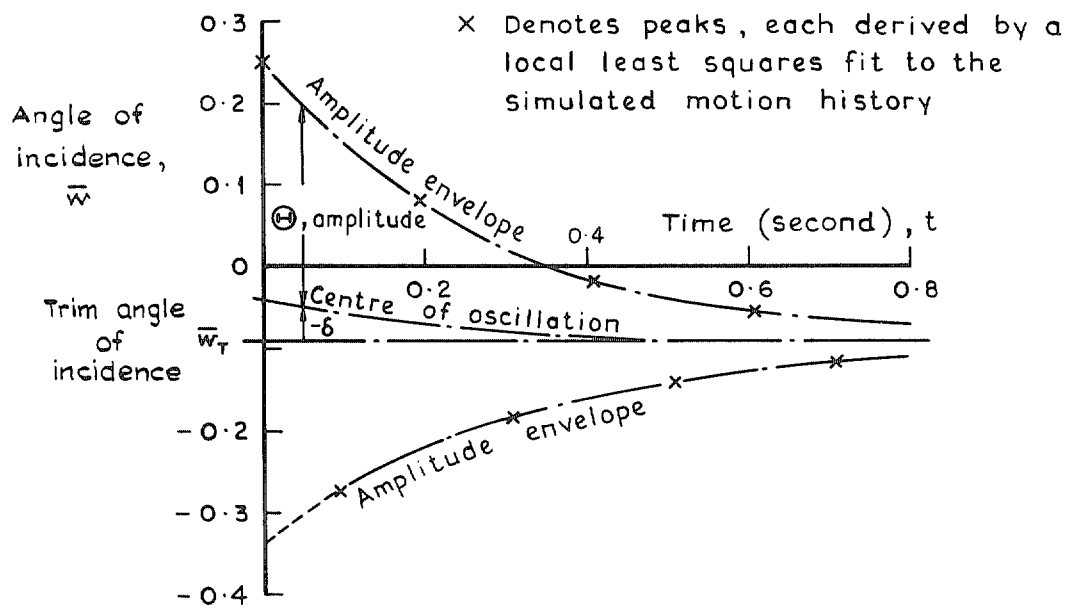

Preliminary stage in computer analysis

Configuration 7, Mach number 2·0, control setting 5 degrees, initial angle of incidence, $\bar{w}_i = 0{\cdot}25$

FIG. 3. Steps in routine analysis of a simulated-response history.

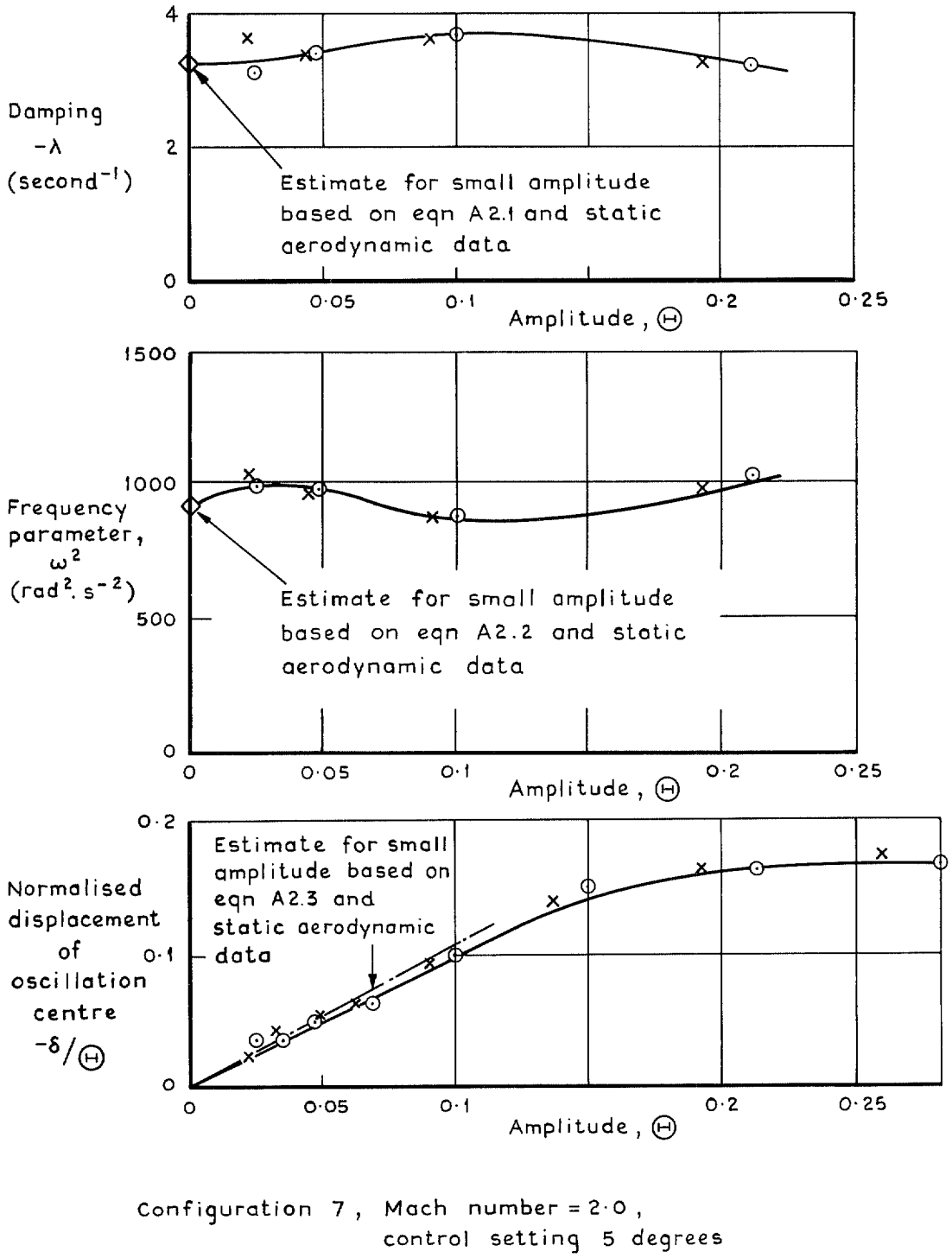

FIG. 4. Dynamic-motion characteristics from analysis of simulated-response histories.

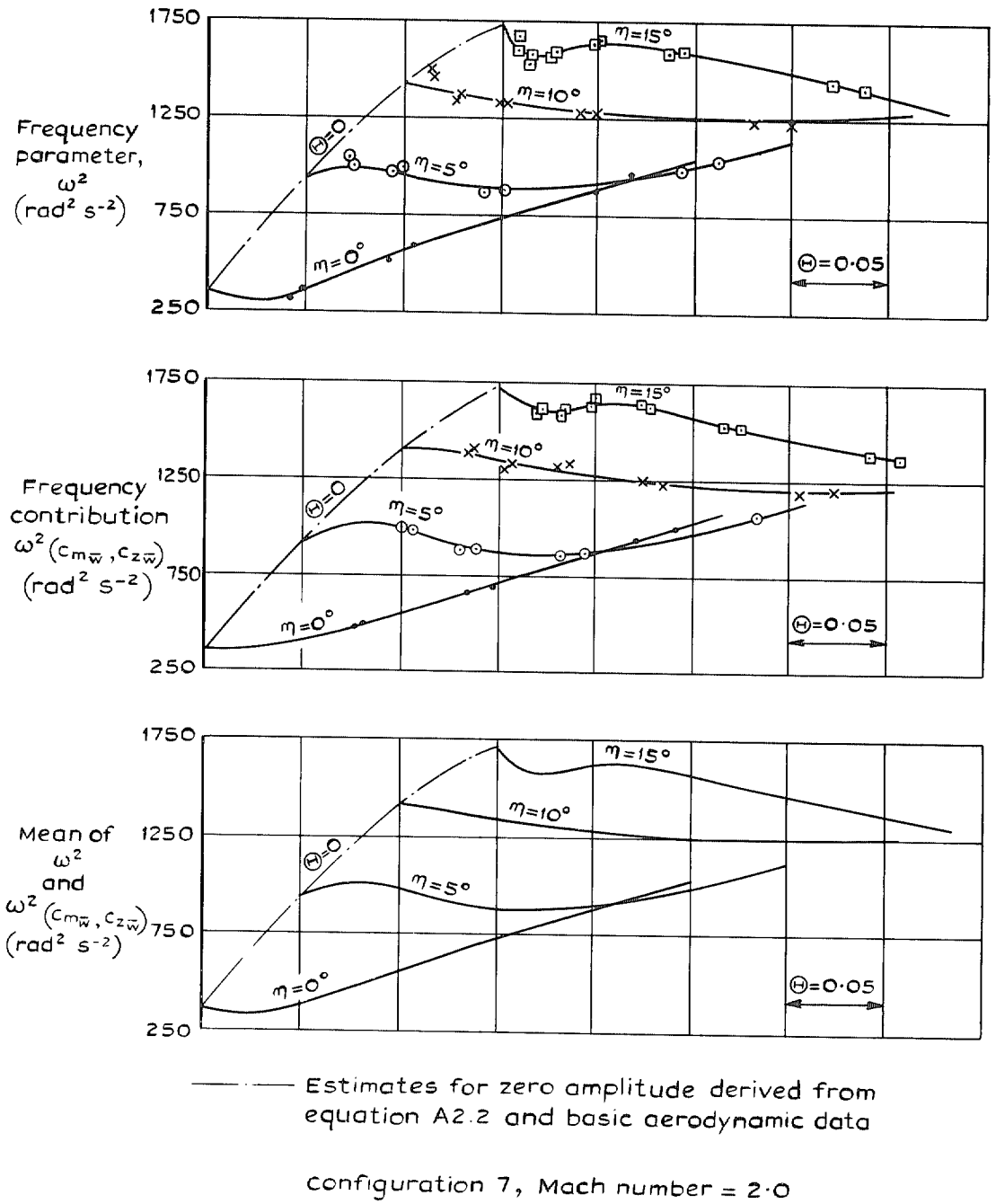

FIG. 5. Presentation of analysed results for frequency parameter as mean of ω^2 and $\omega^2_{(C_{m\bar{w}}, C_{z\bar{w}})}$.

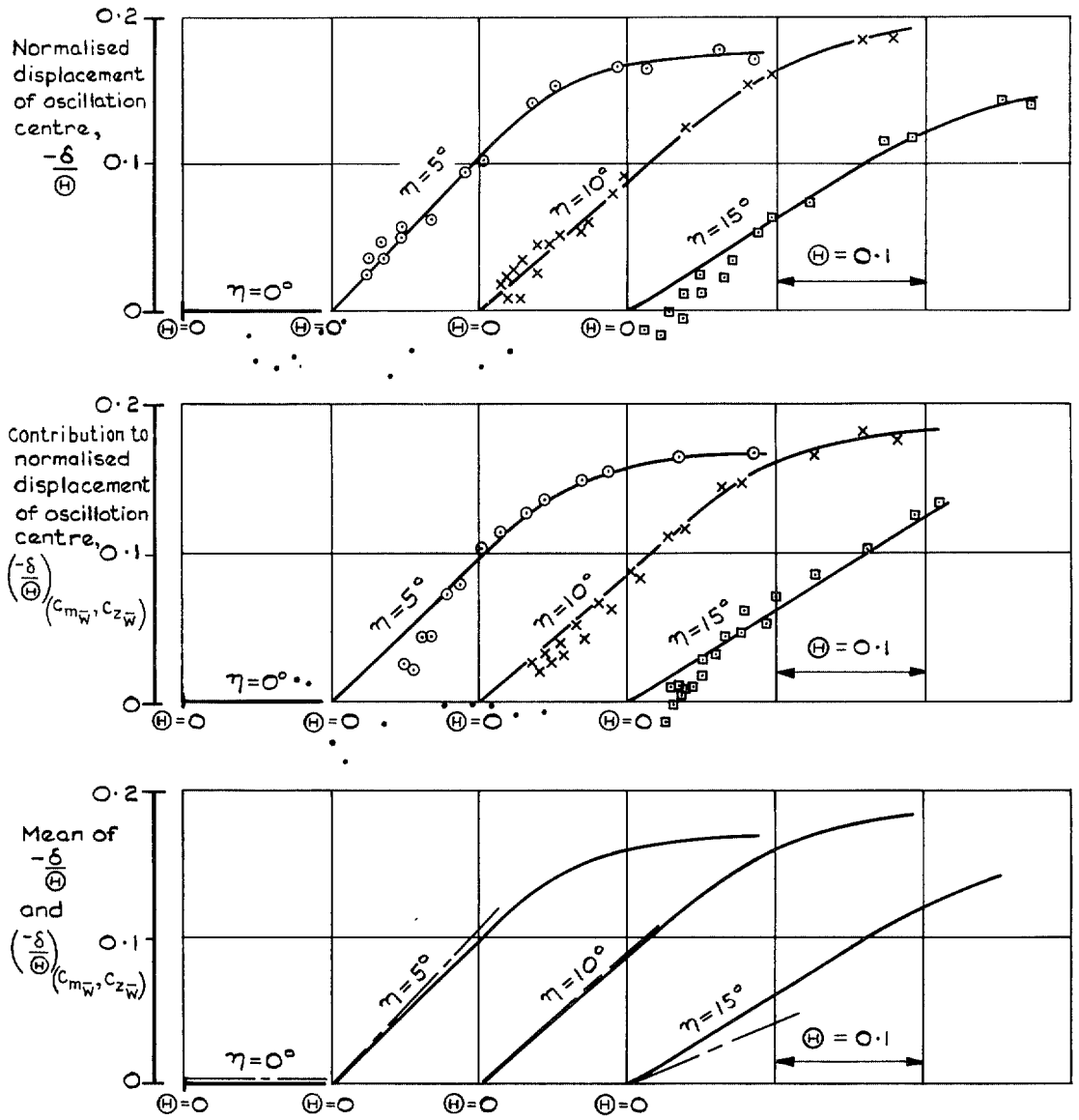

FIG. 6. Combined presentation of displacement of oscillation centre, δ/Θ and $(\delta/\Theta)_{(C_{m_{\bar{w}}}, C_{z_{\bar{w}}})}$, with correction in region of small amplitude.

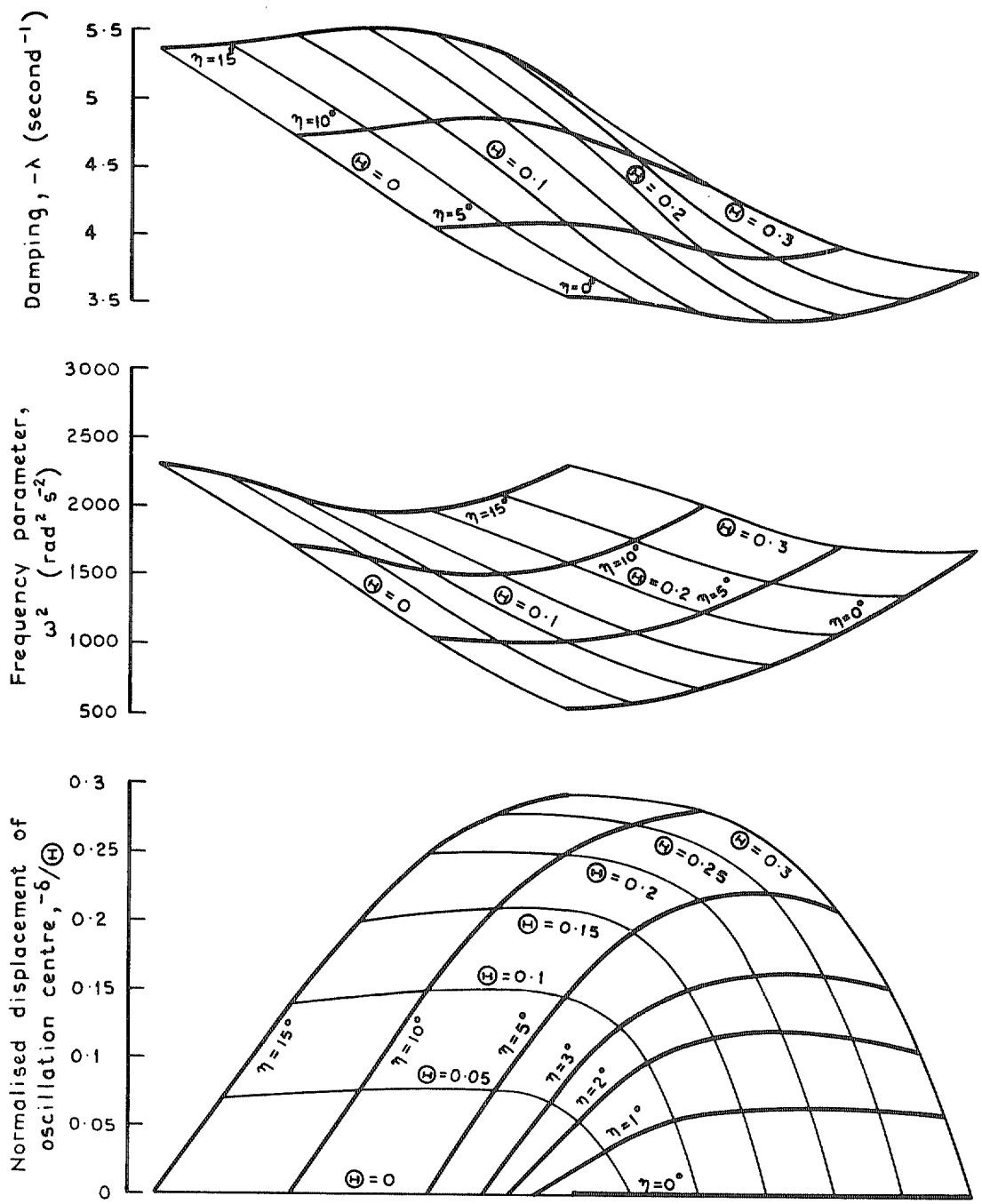

FIG. 7. Theoretical characteristics for an idealised flight vehicle with 'hard' aerodynamic form (form 3 of Ref. 5).

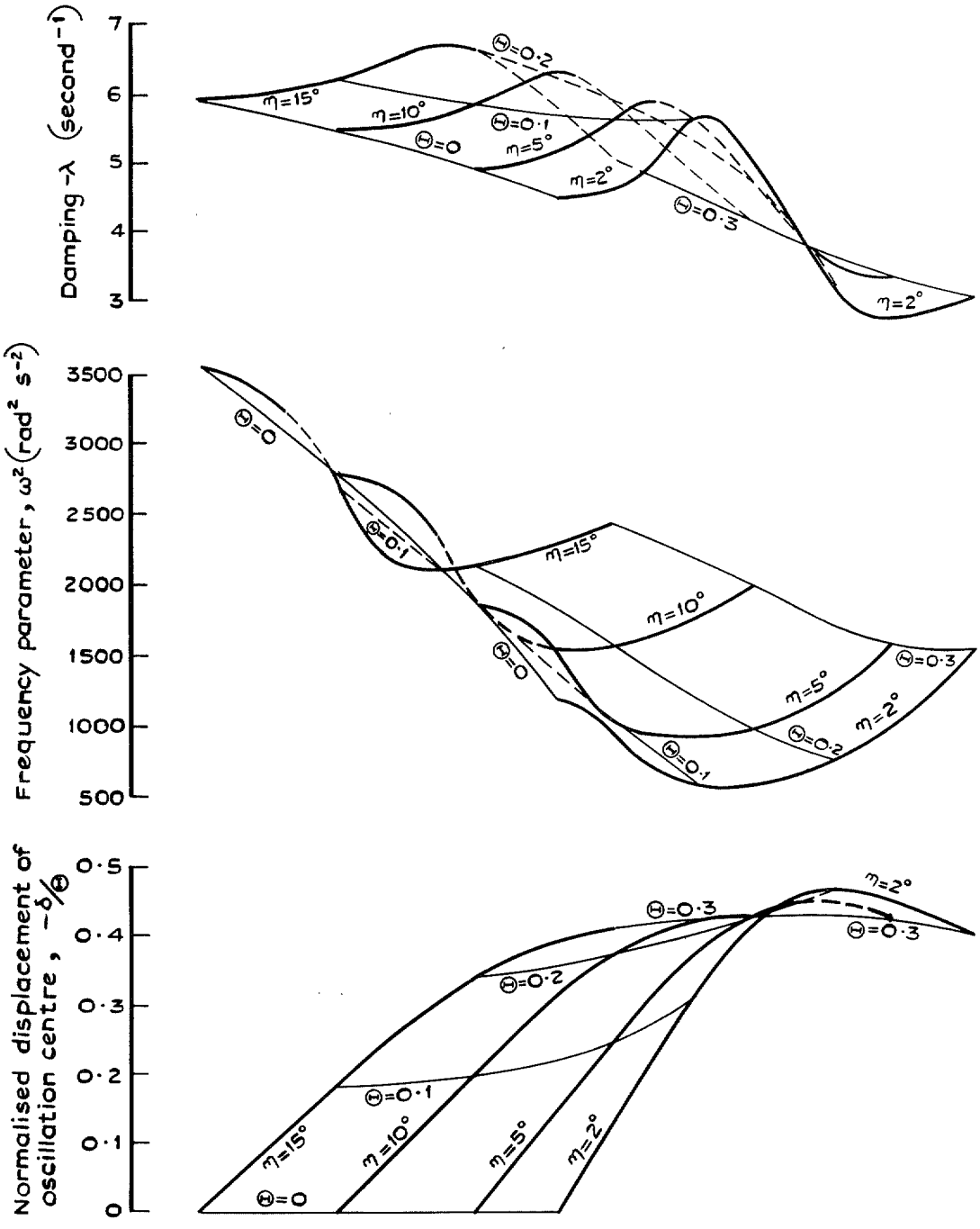

FIG. 8. Theoretical characteristics for an idealised flight vehicle with aerodynamic form destabilising for small angles of incidence (form 6 of Ref. 5).

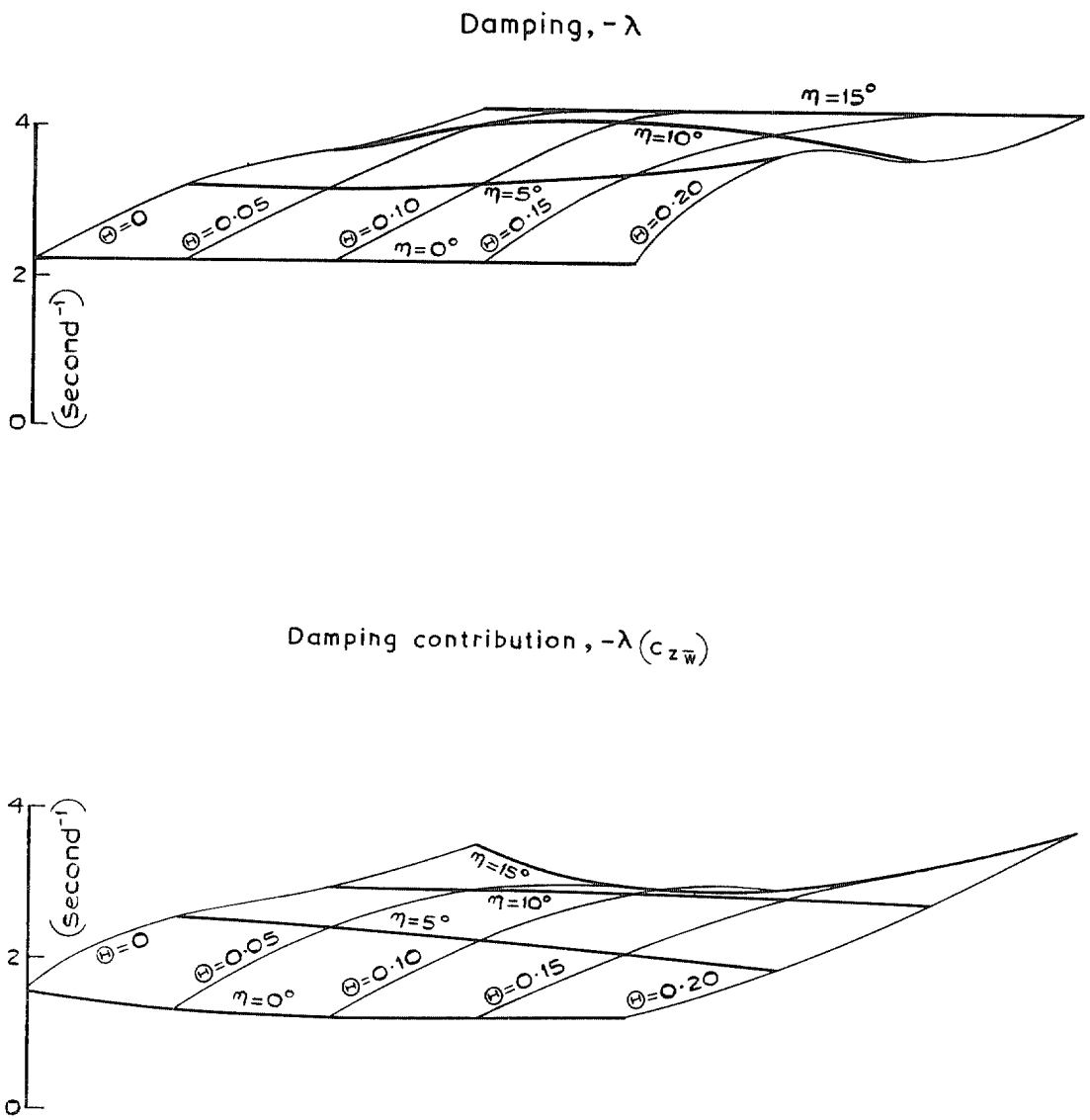

FIG. 9. Configuration 1—dynamic characteristics for $M = 1{\cdot}6$.

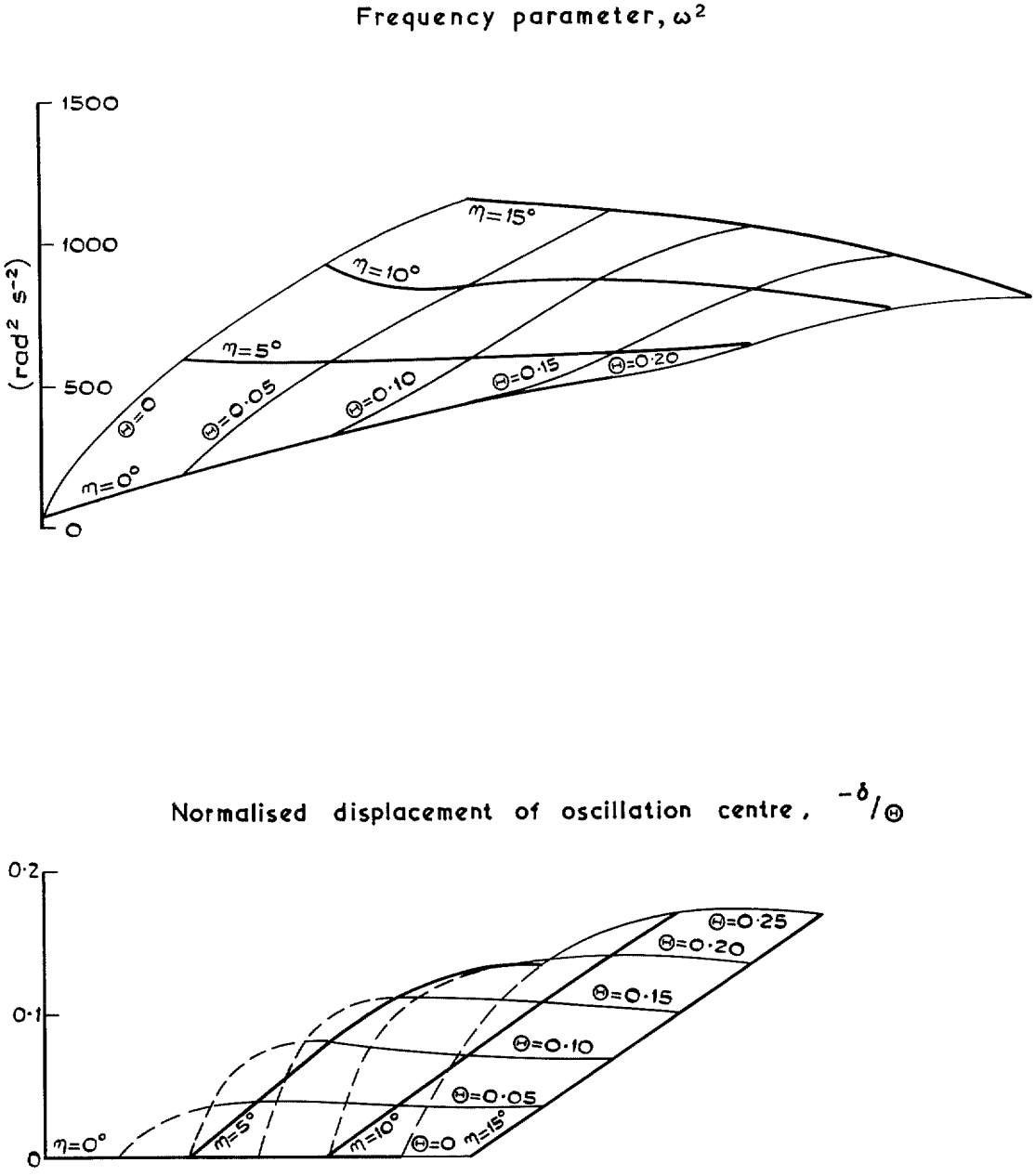

FIG. 9—continued.

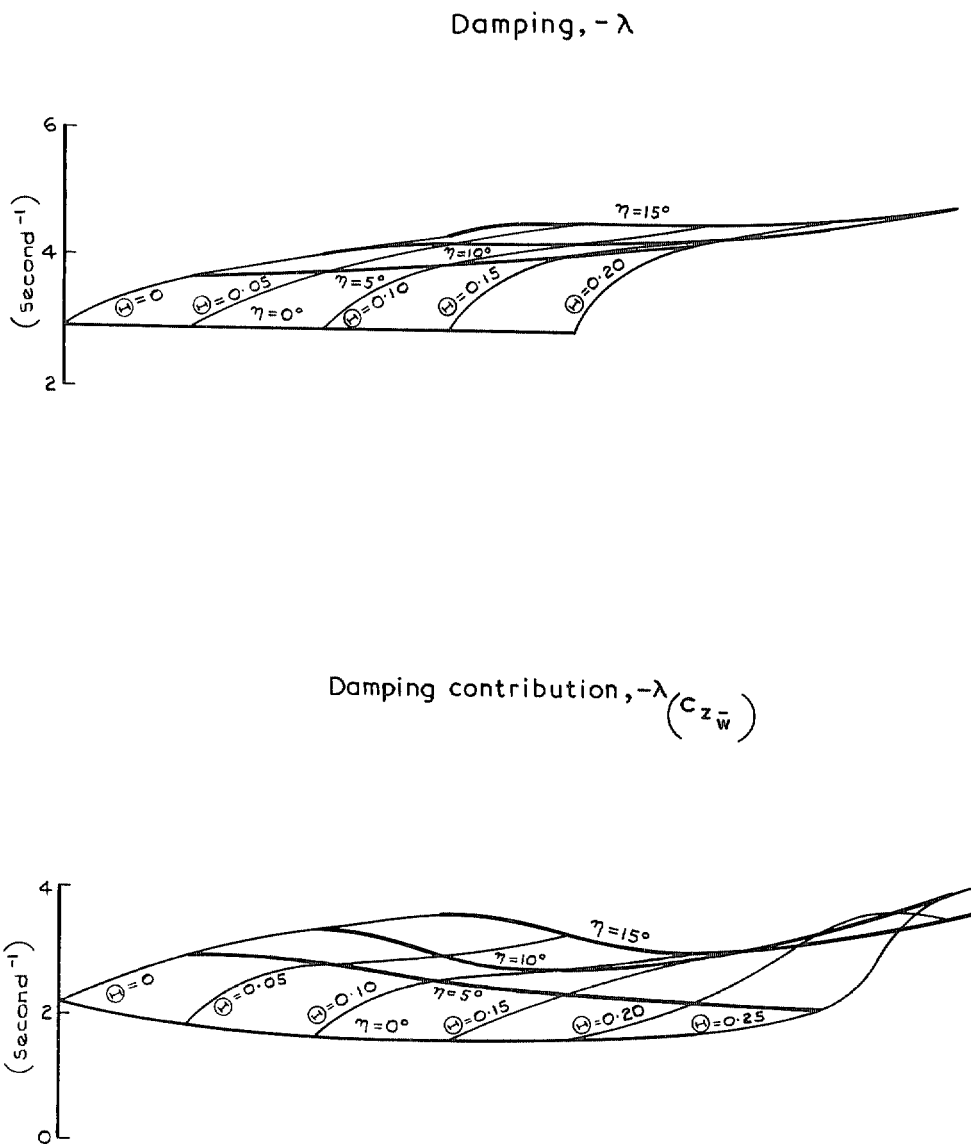

FIG. 10. Configuration 1—dynamic characteristics for $M = 2{\cdot}0$.

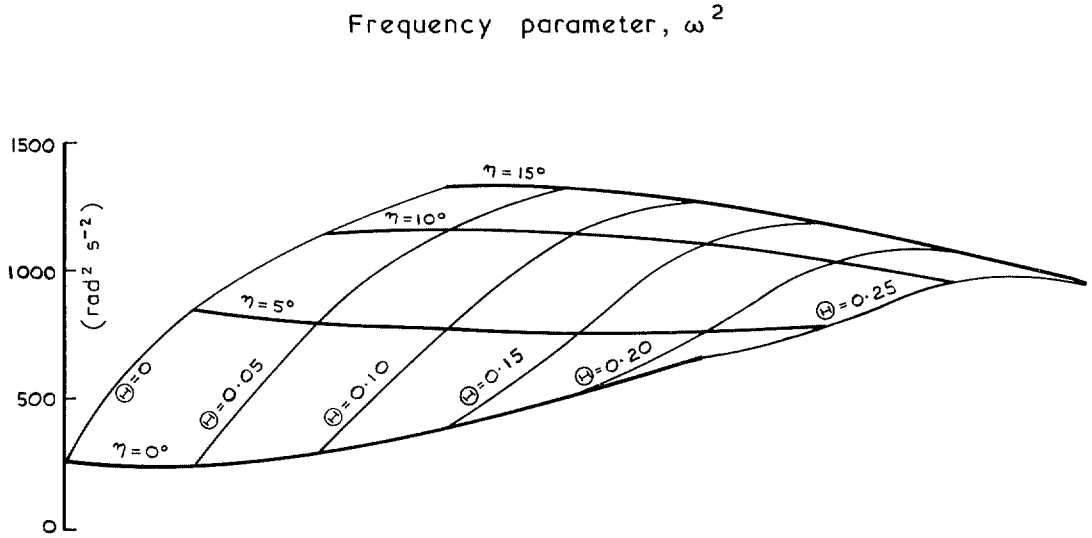

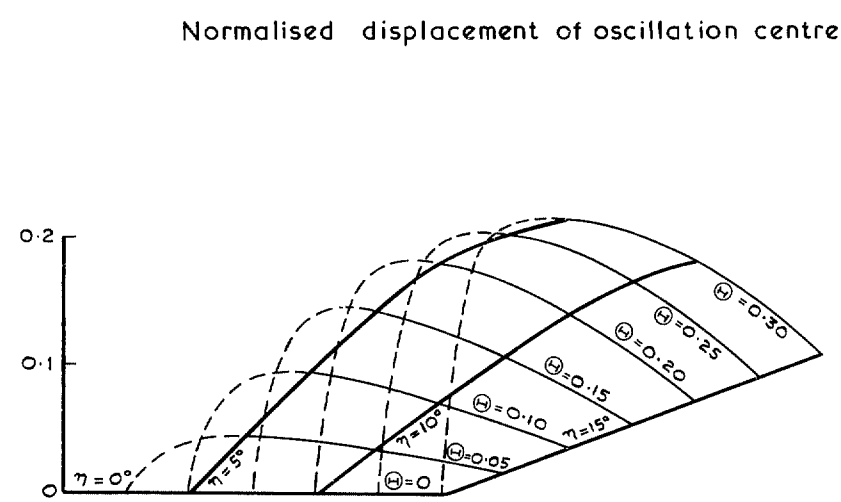

FIG. 10—continued.

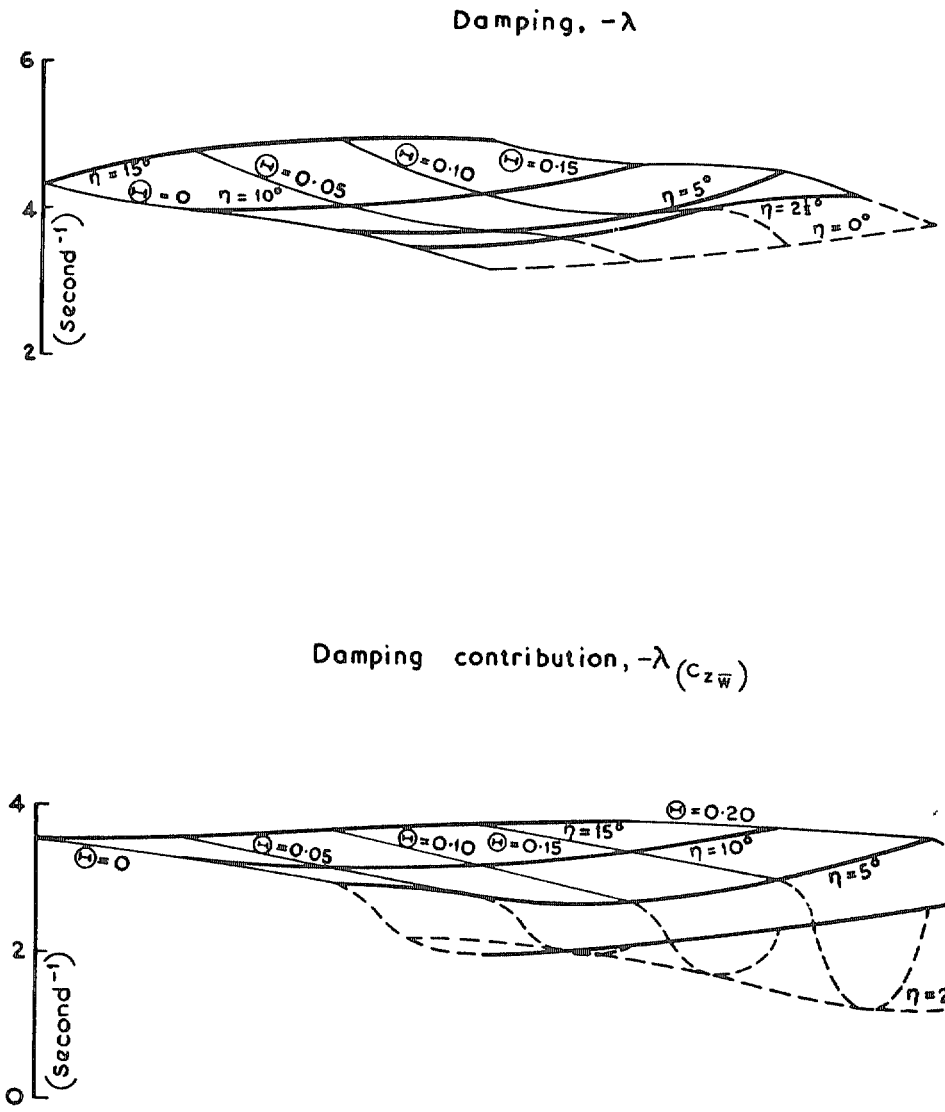

FIG. 11. Configuration 2F—dynamic characteristics for $M = 1{\cdot}6$.

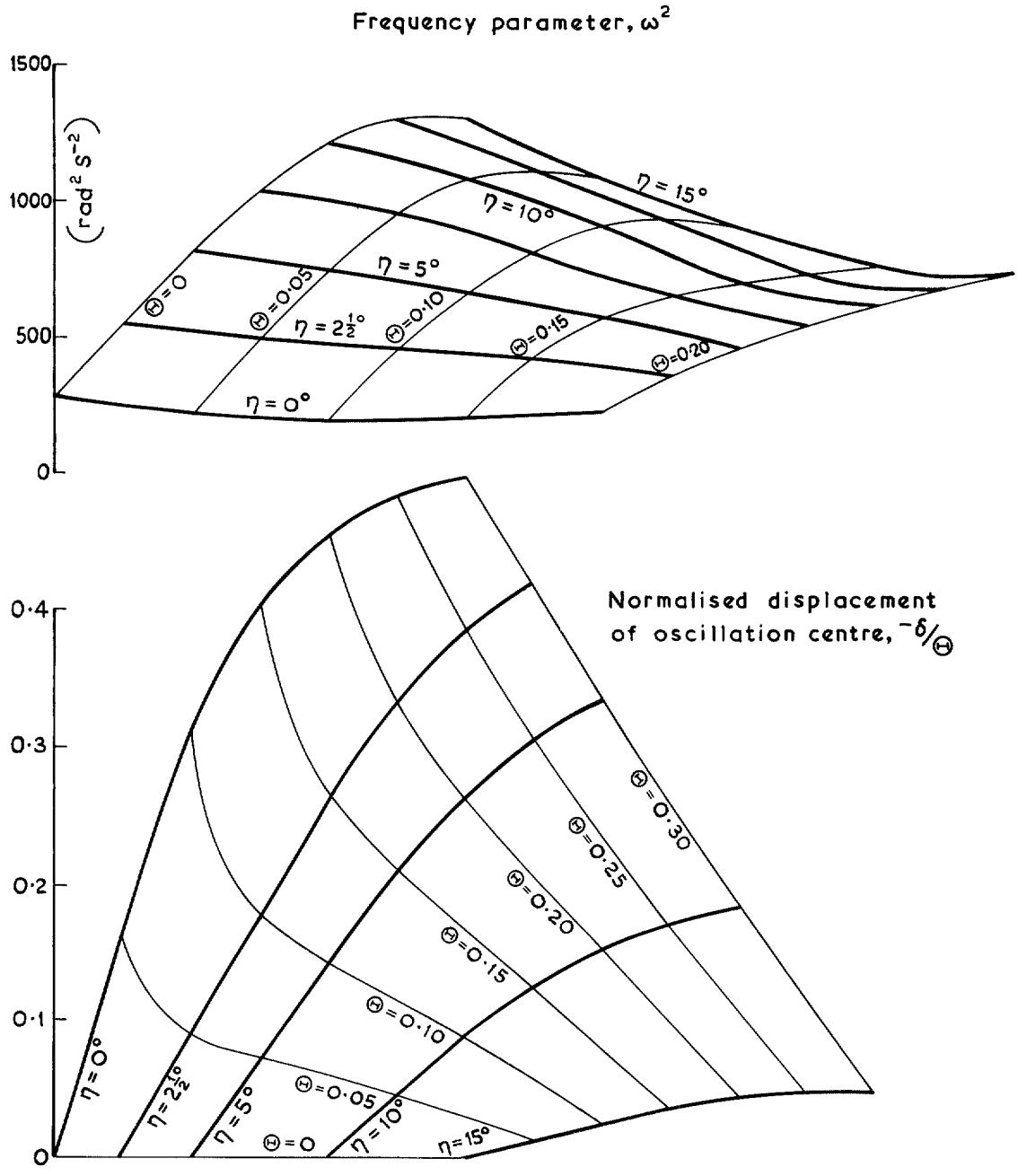

FIG. 11—continued.

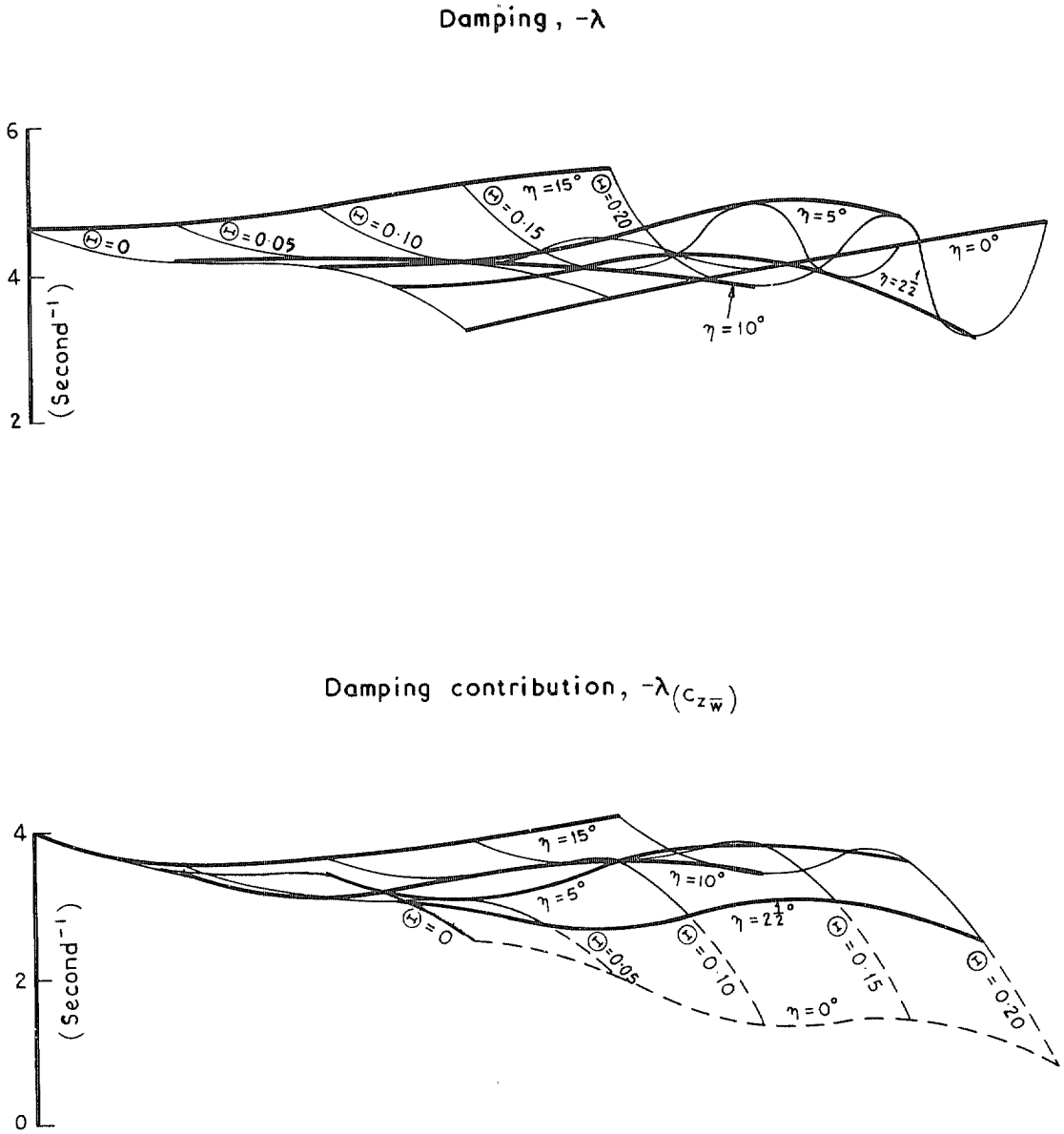

FIG. 12. Configuration 2F—dynamic characteristics for $M = 2{\cdot}0$.

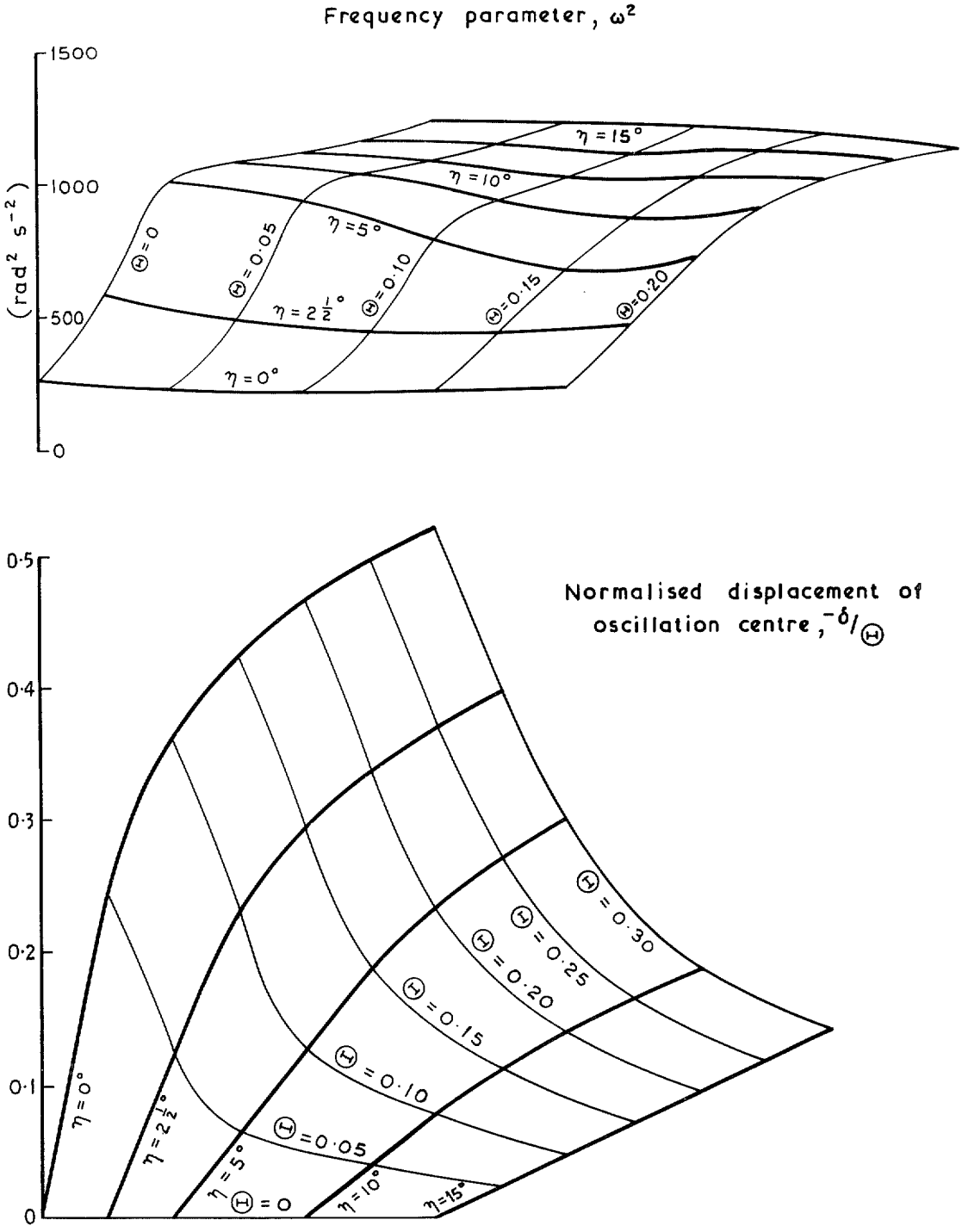

FIG. 12—continued.

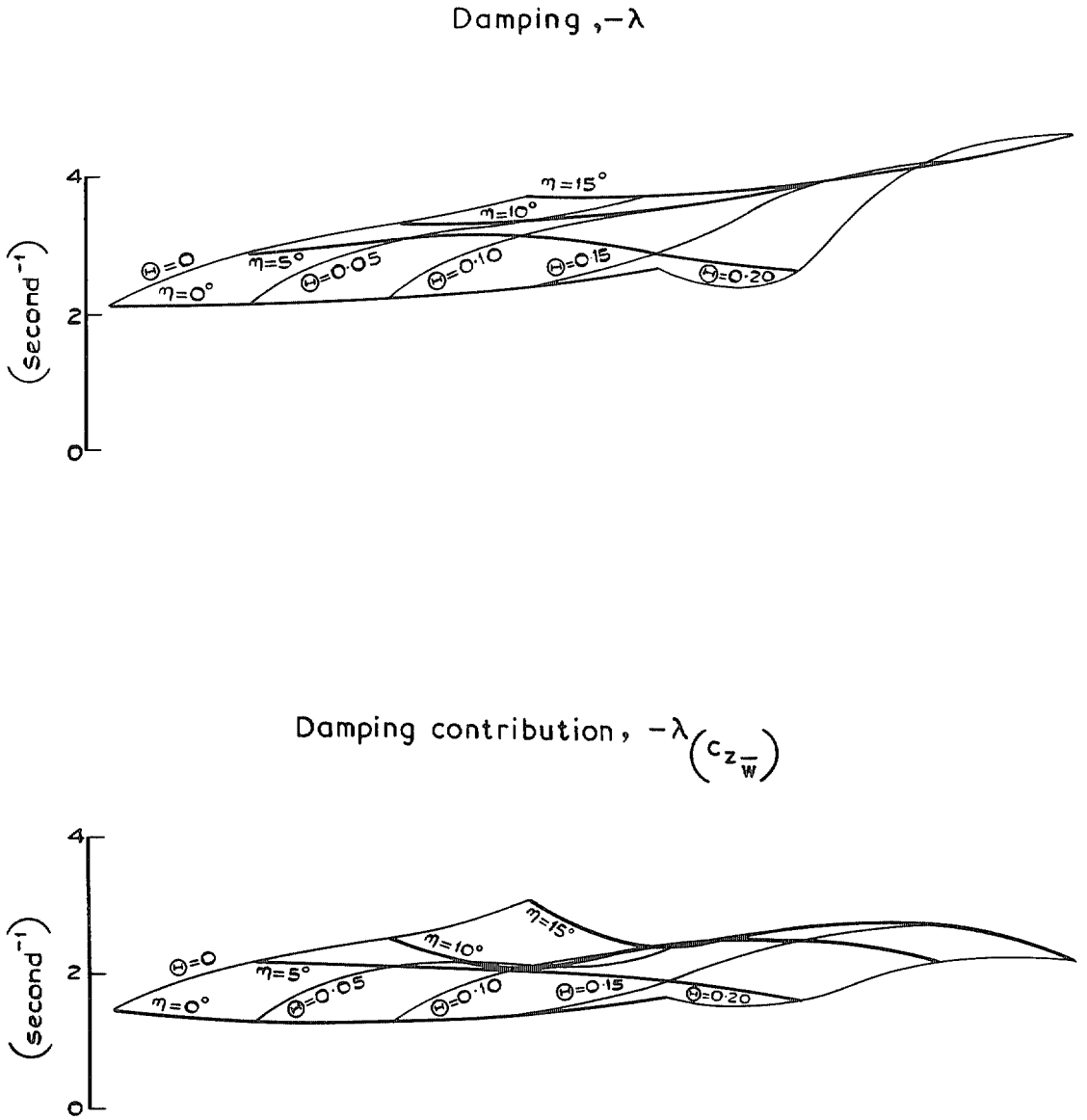

FIG. 13. Configuration 2R —dynamic characteristics for $M = 1{\cdot}6$.

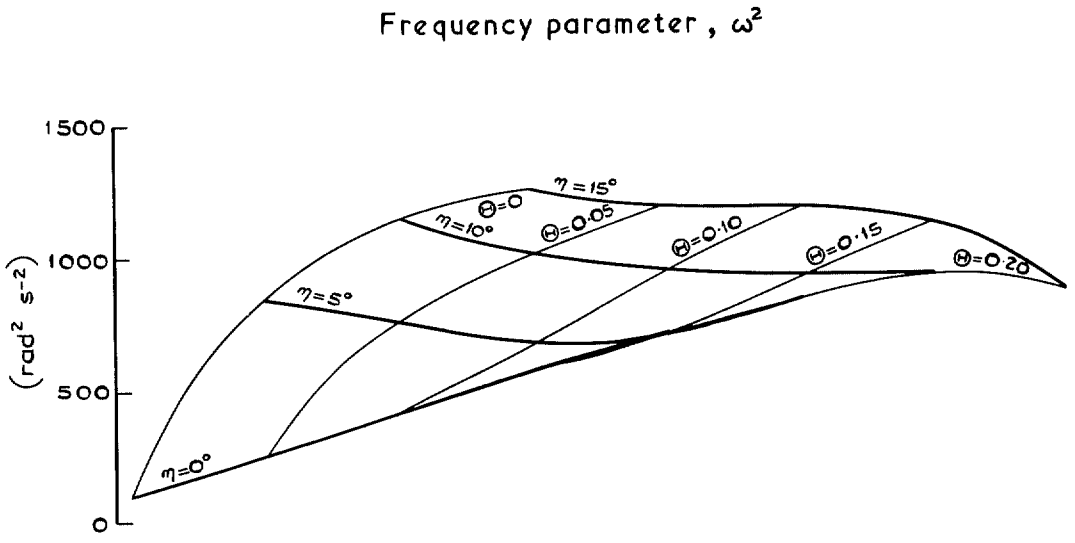

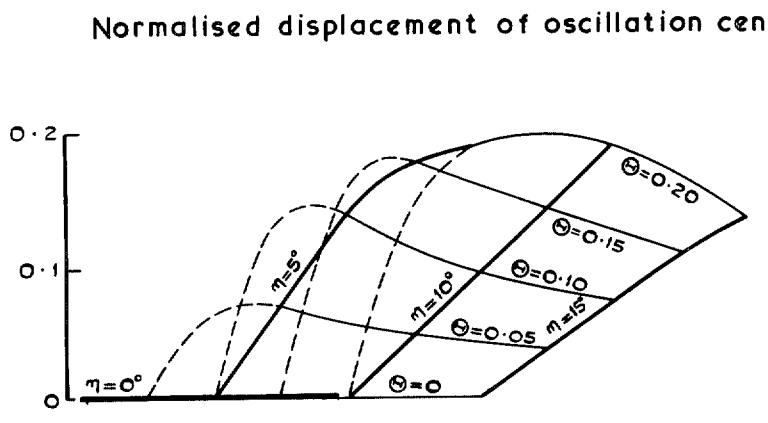

FIG. 13—continued.

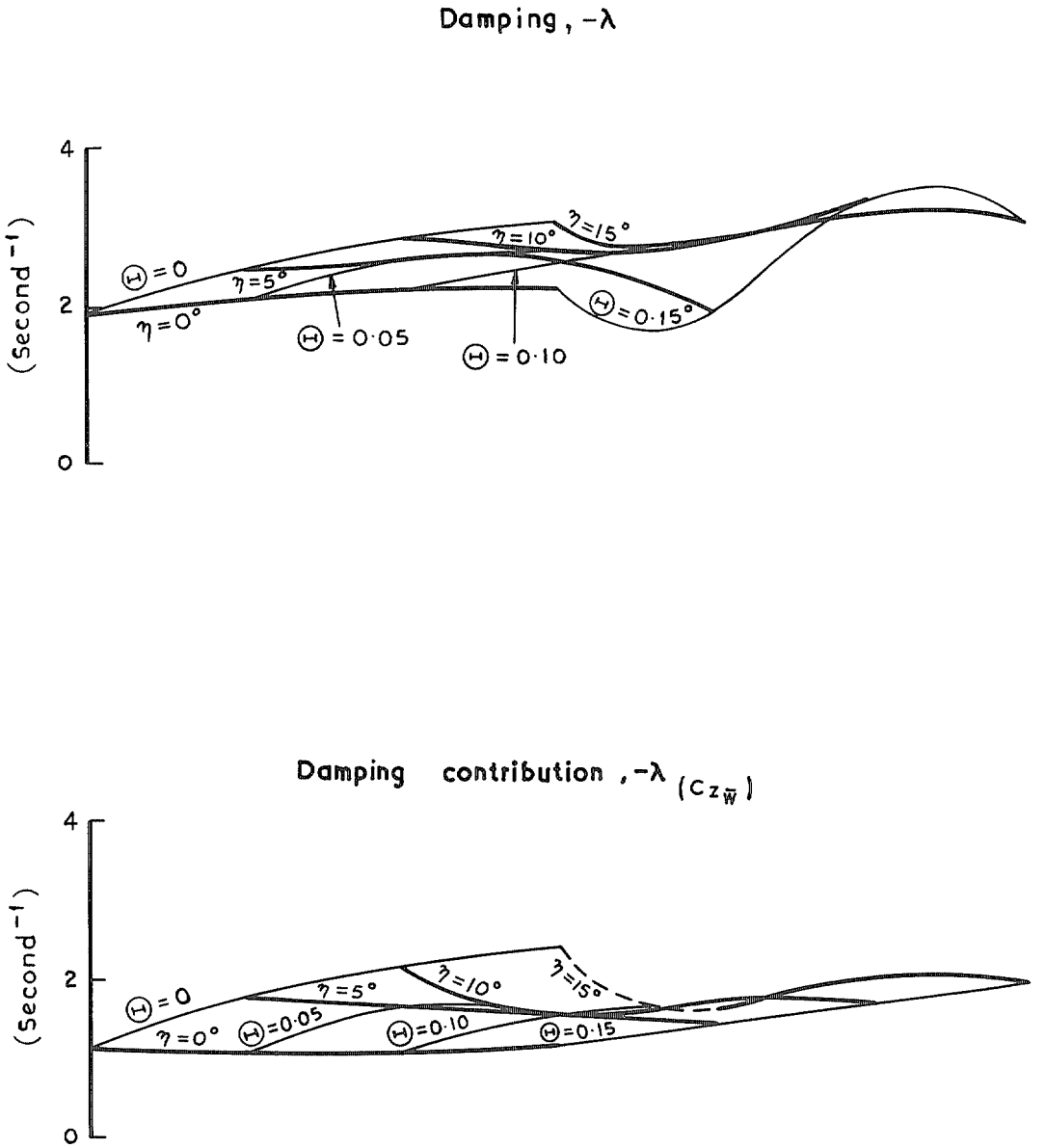

FIG. 14. Configuration 3—dynamic characteristics for $M = 1{\cdot}6$.

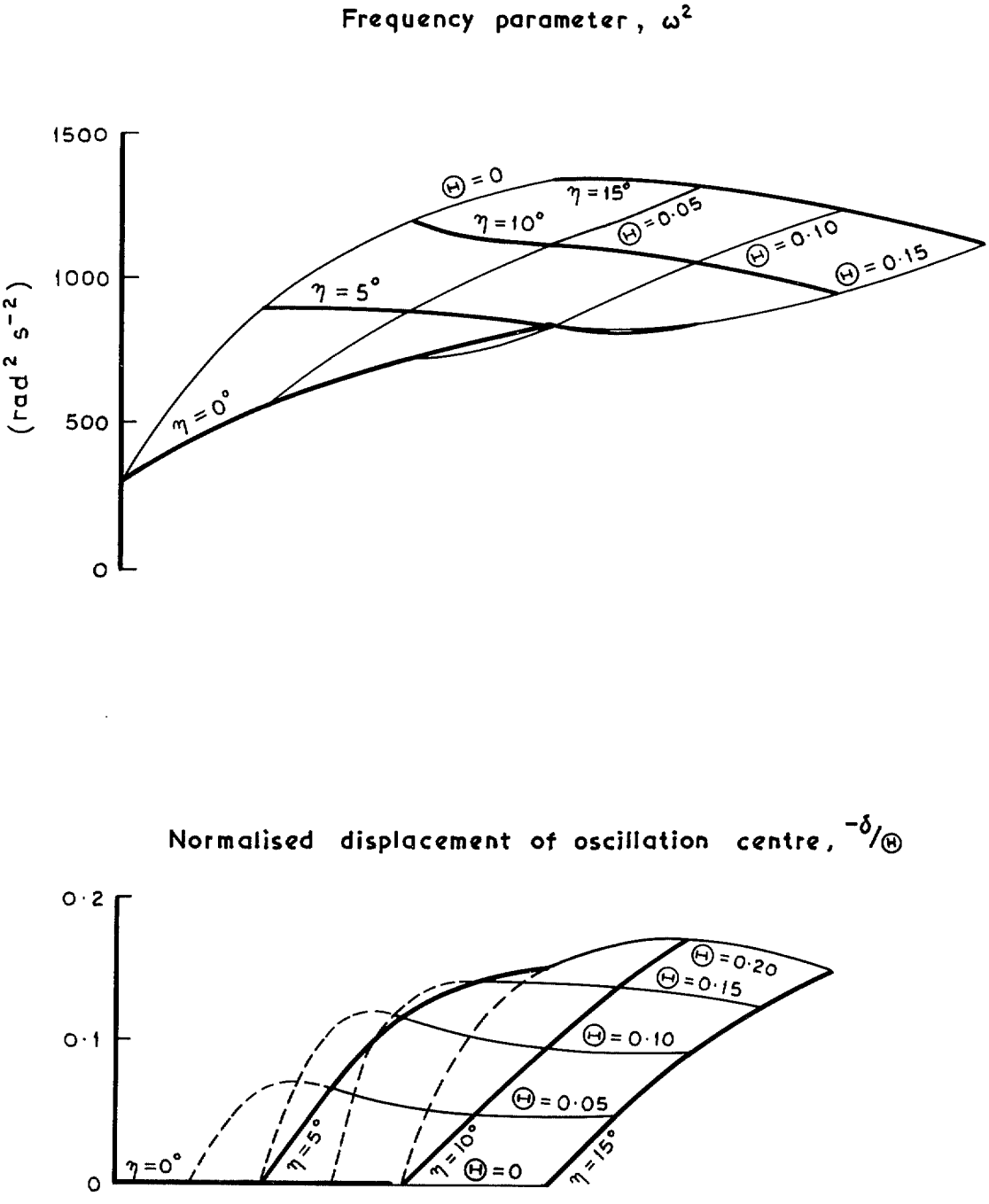

FIG. 14—continued.

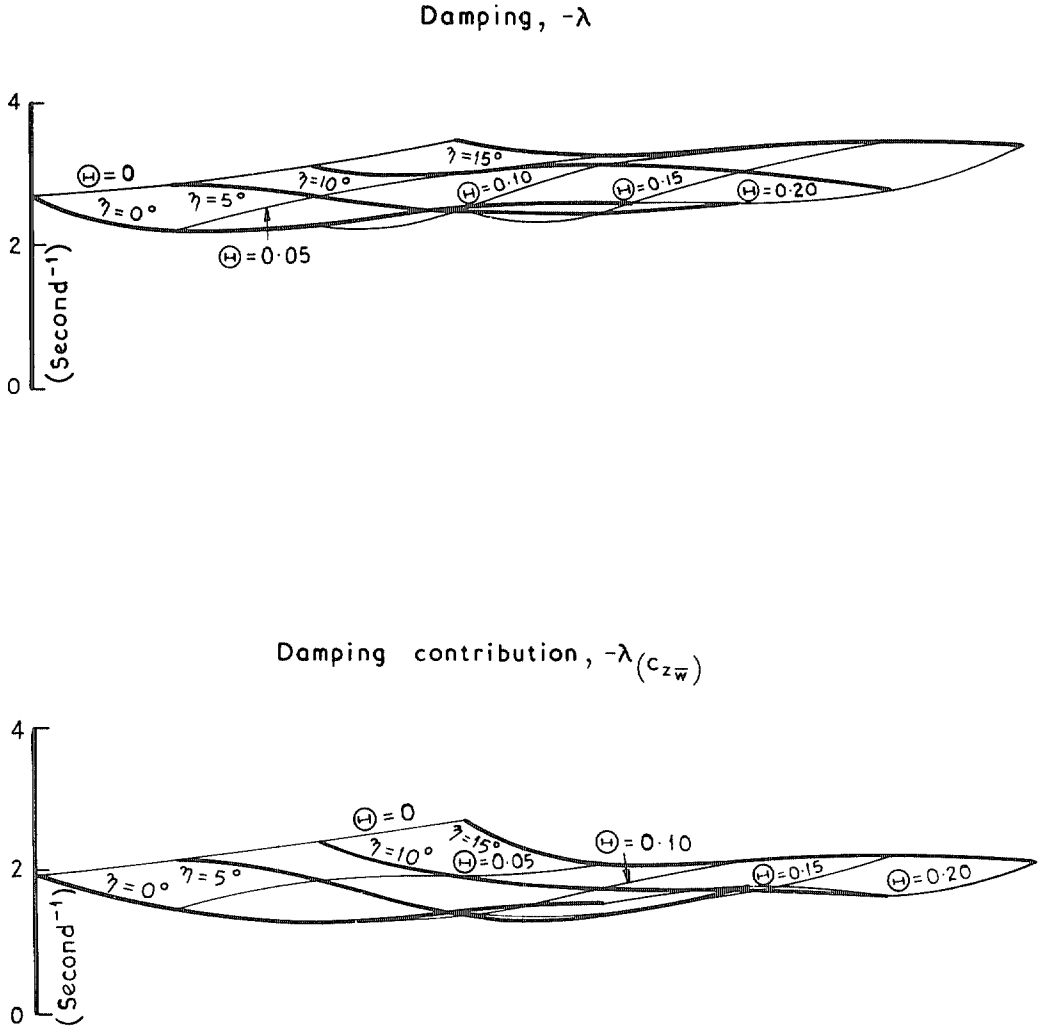

FIG. 15. Configuration 3—dynamic characteristics for $M = 2{\cdot}0$.

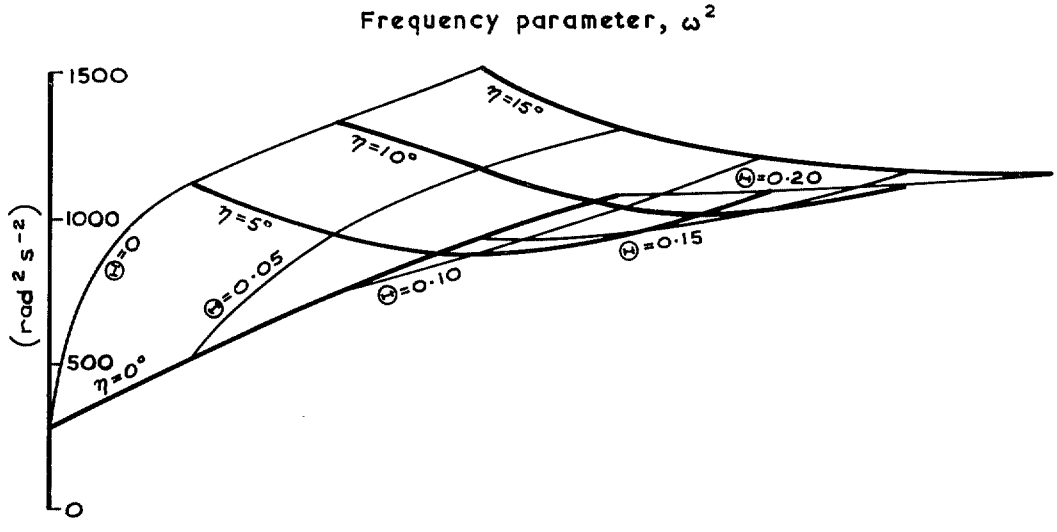

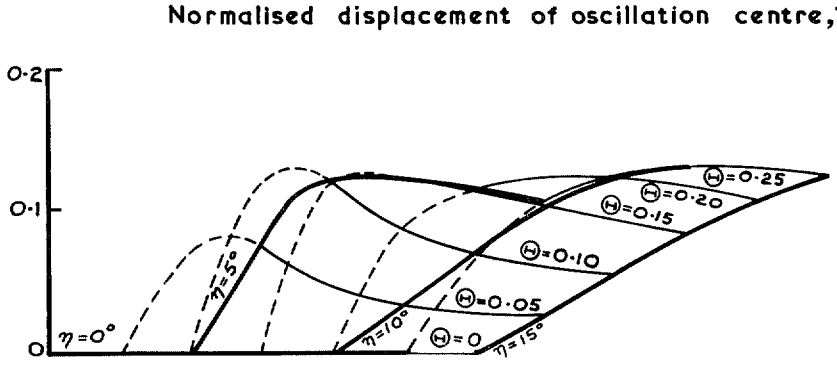

FIG. 15—continued.

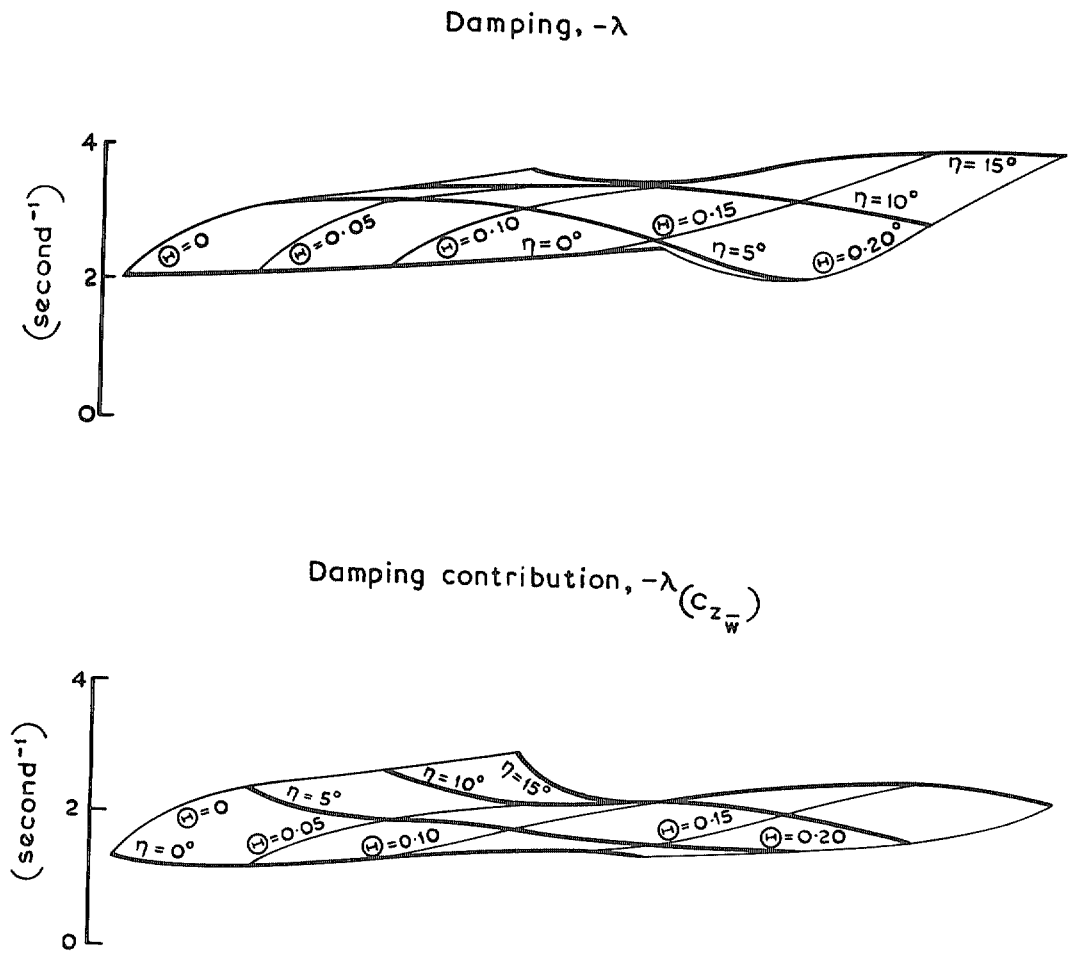

FIG. 16. Configuration 4—dynamic characteristics for $M = 1{\cdot}6$.

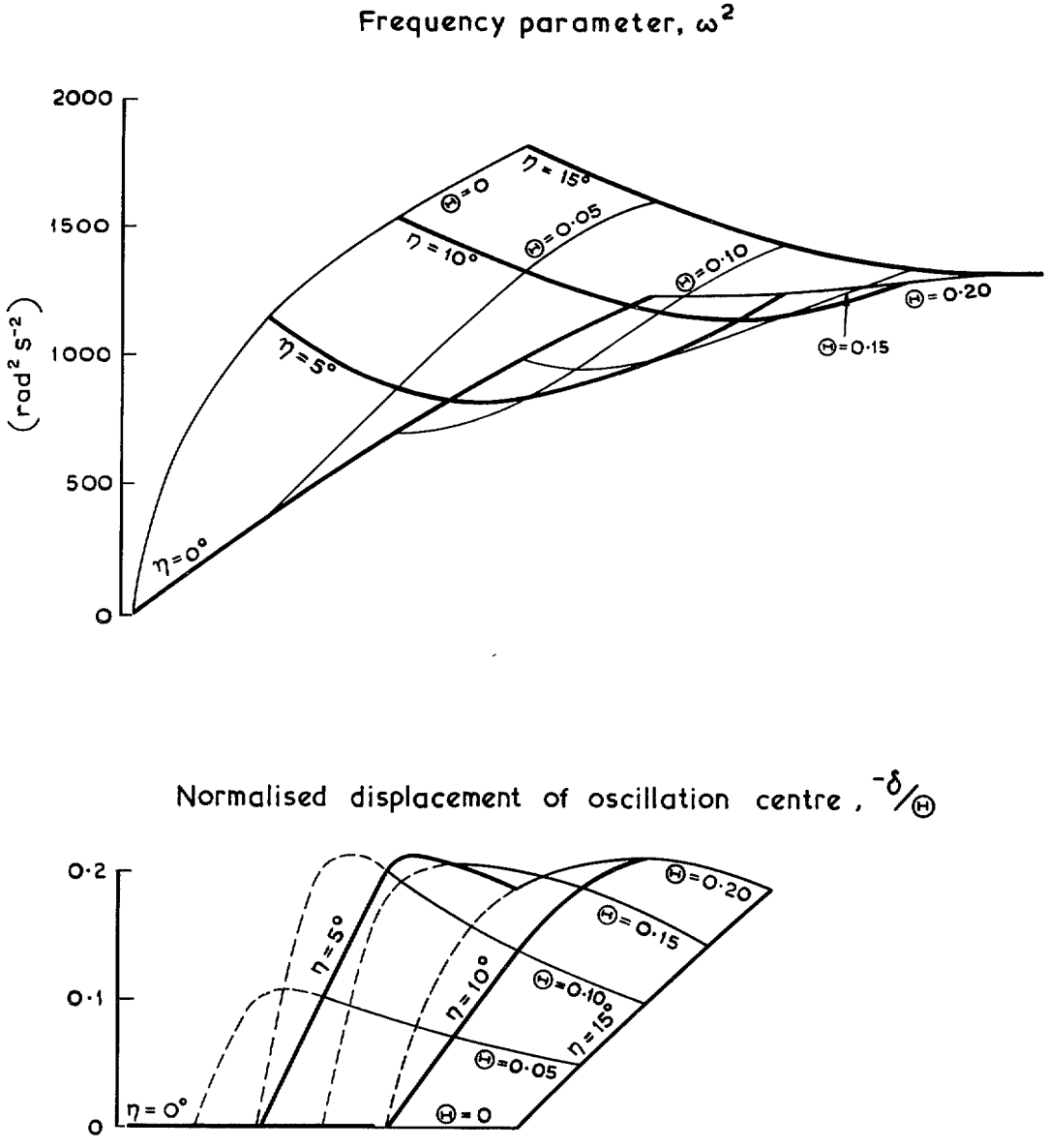

FIG. 16—continued.

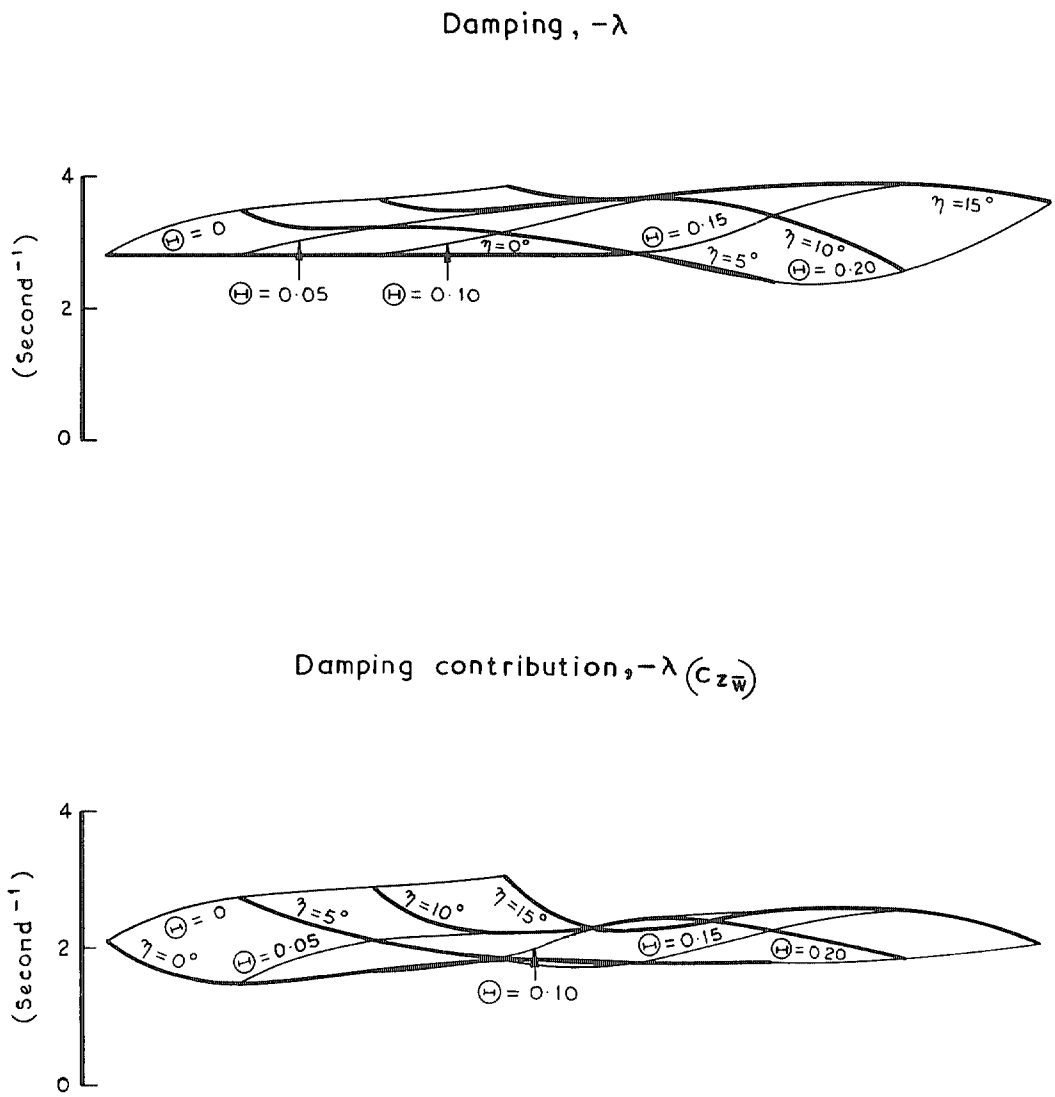

FIG. 17. Configuration 4—dynamic characteristics for $M = 2{\cdot}0$.

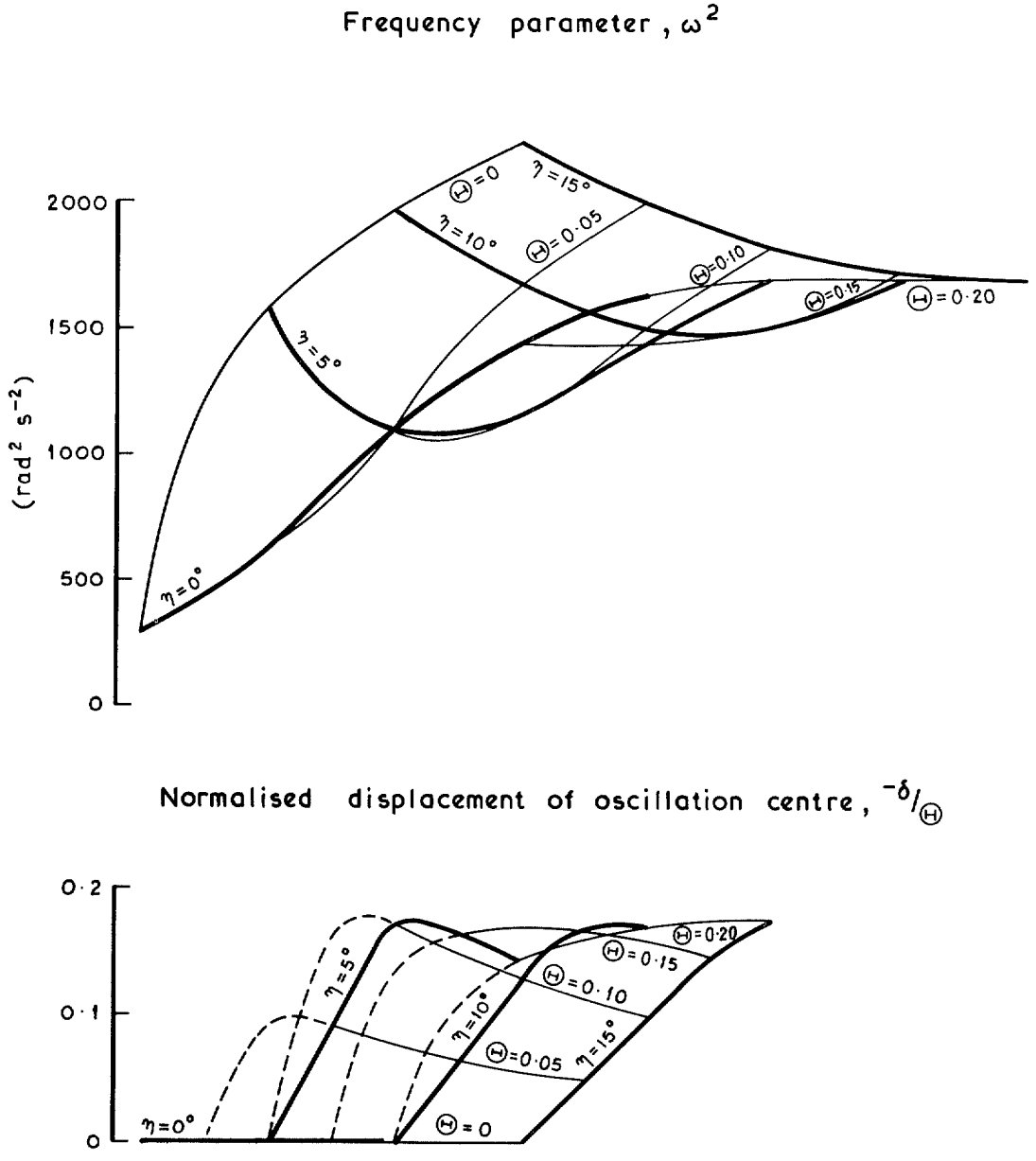

FIG. 17—continued.

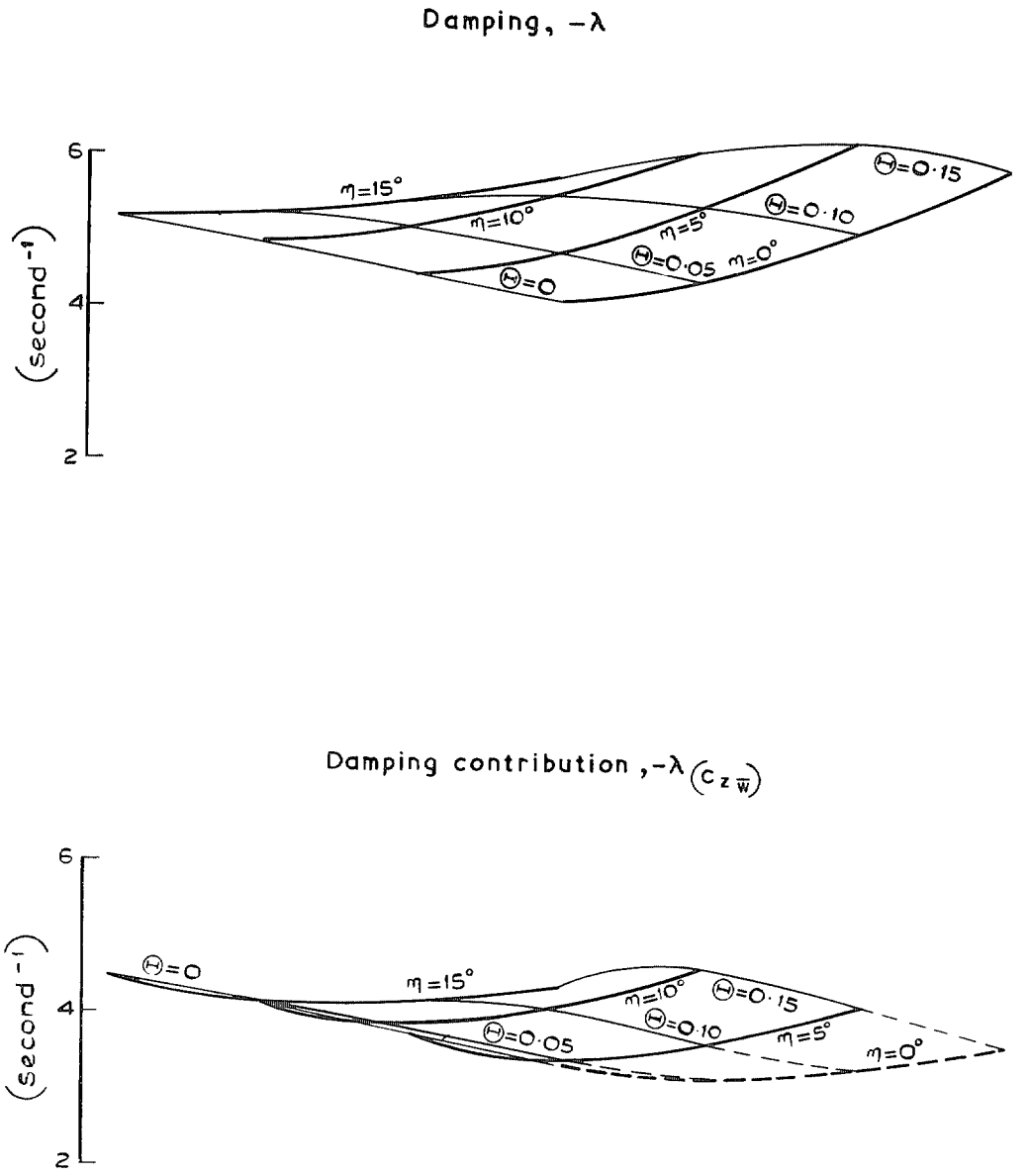

FIG. 18. Configuration 5– dynamic characteristics for $M = 1{\cdot}6$.

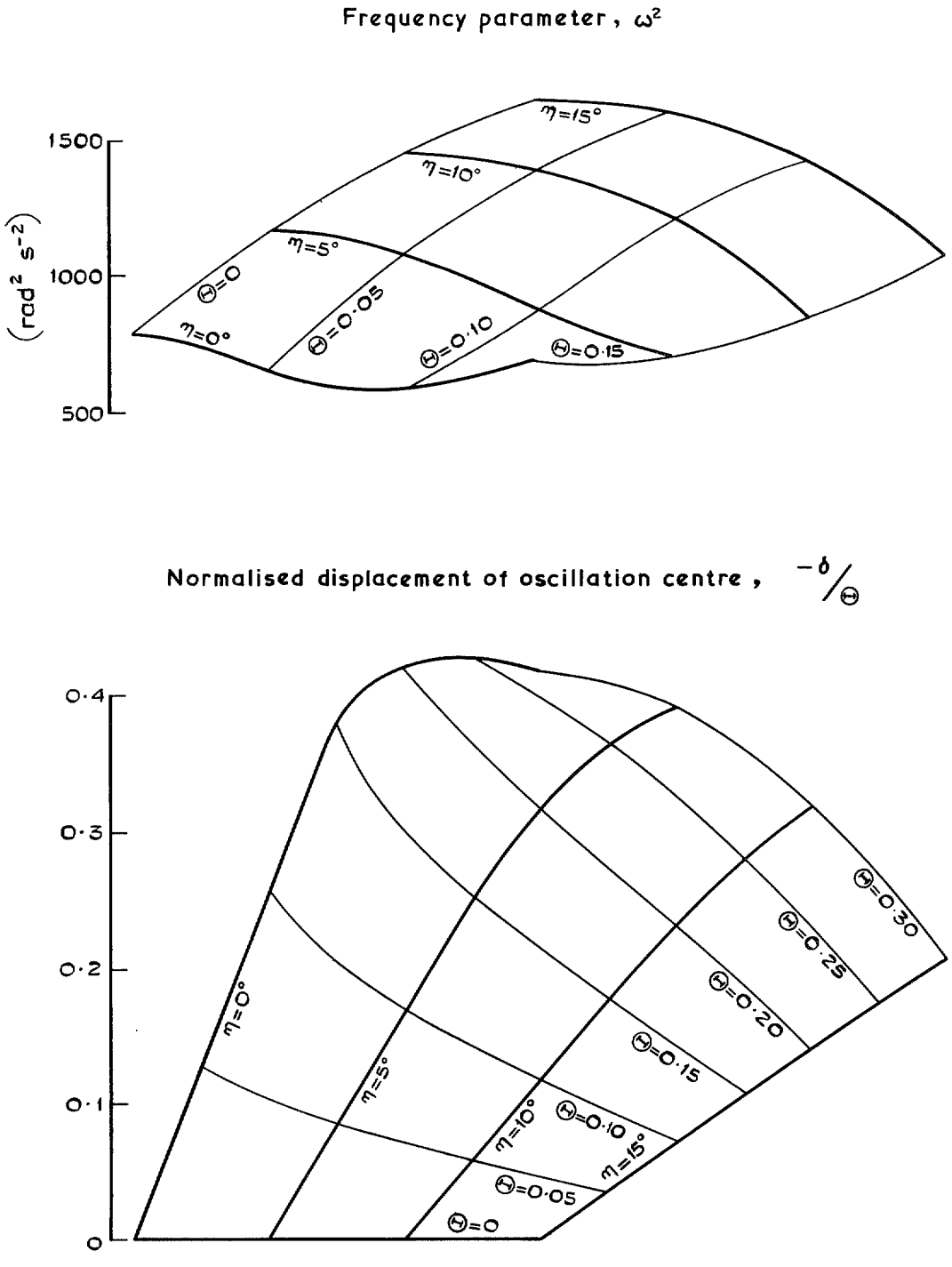

FIG. 18—continued.

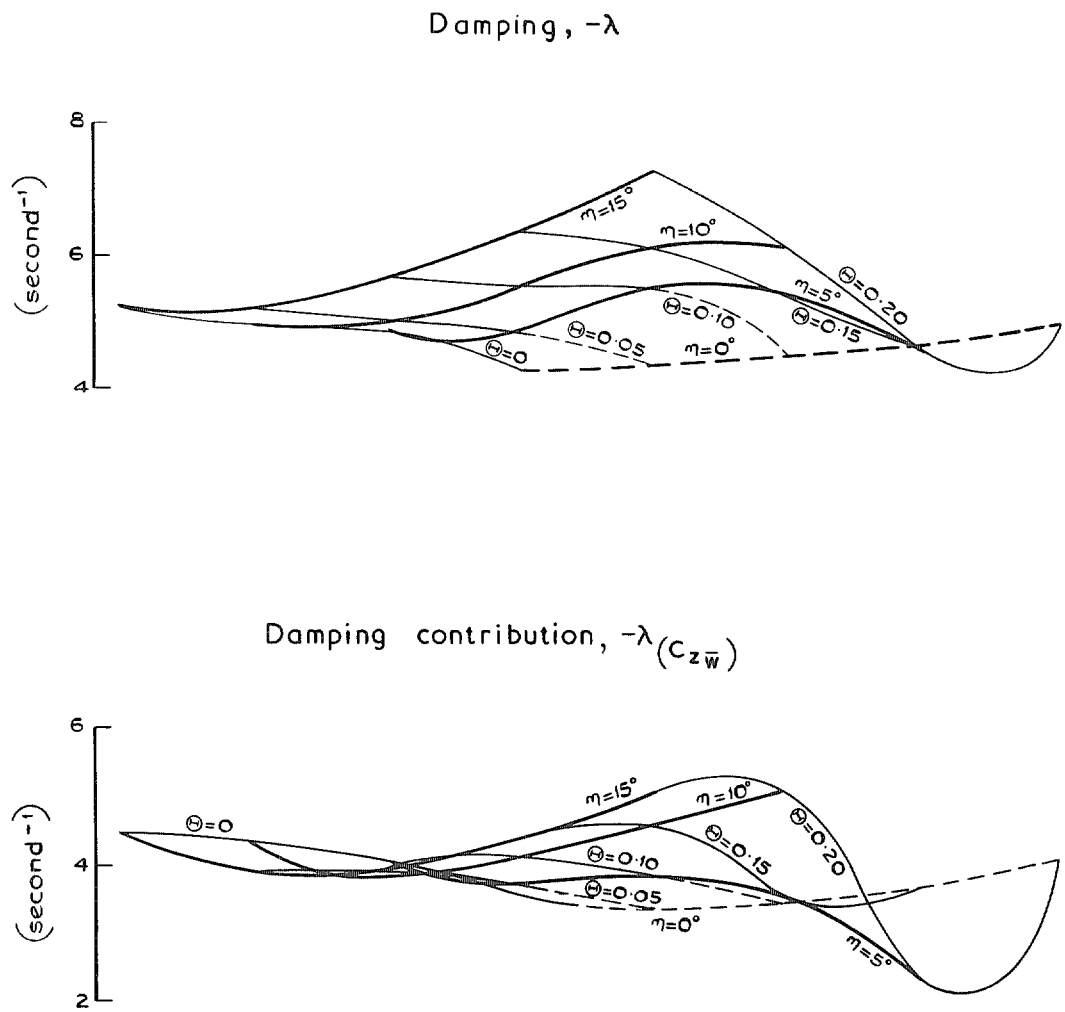

FIG. 19. Configuration 5—dynamic characteristics for $M = 2{\cdot}0$.

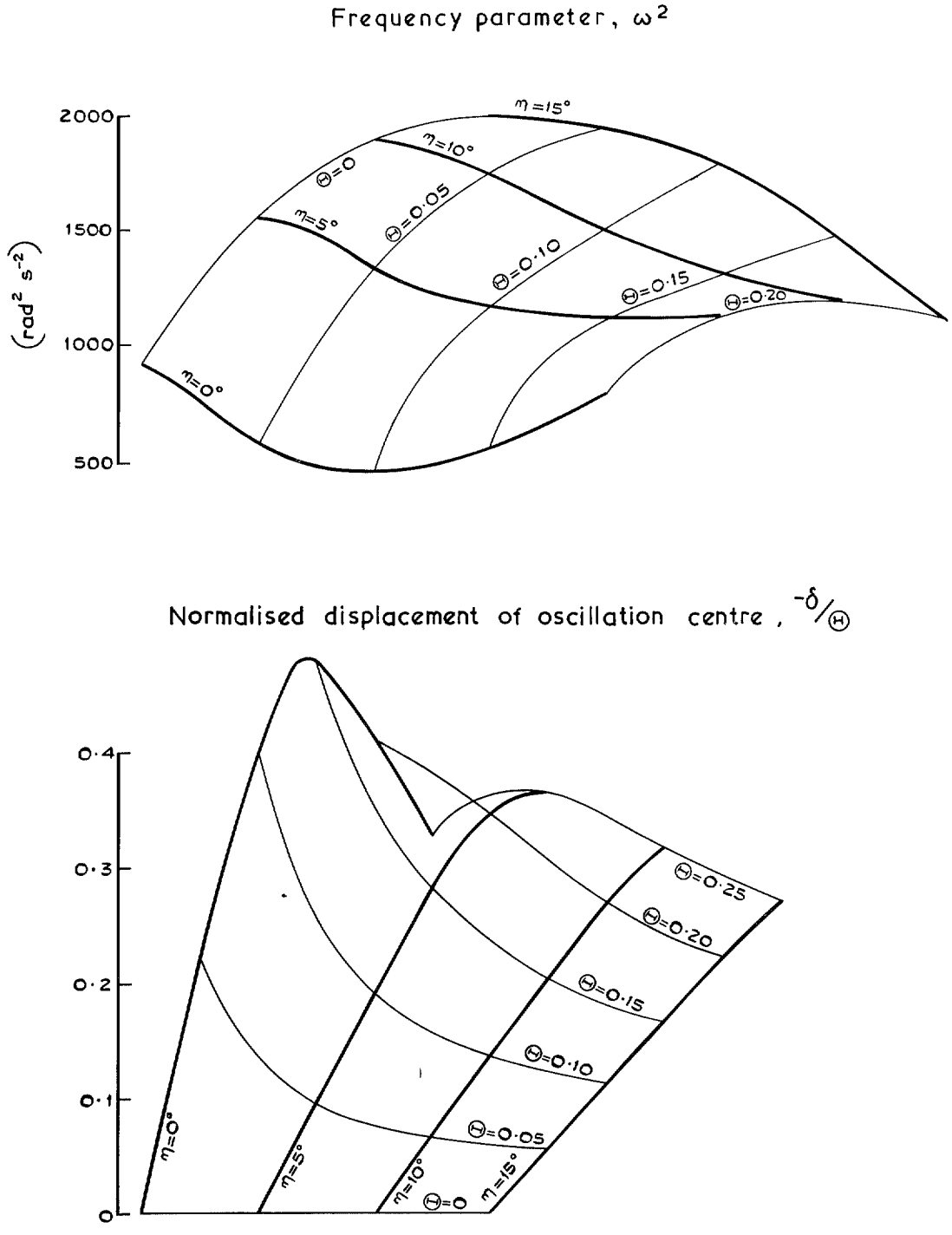

FIG. 19—continued.

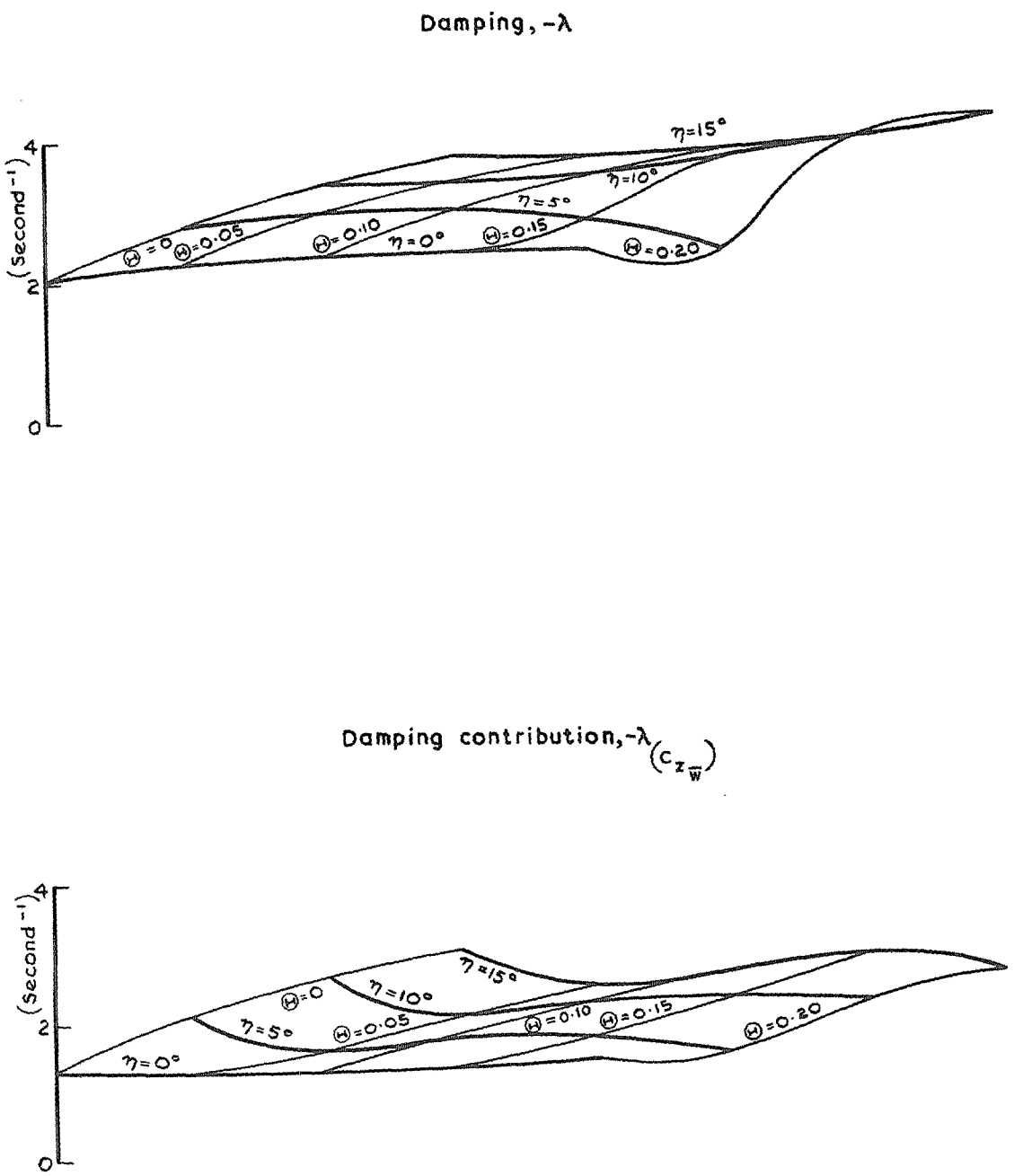

FIG. 20. Configuration 6—dynamic characteristics for $M = 1{\cdot}6$.

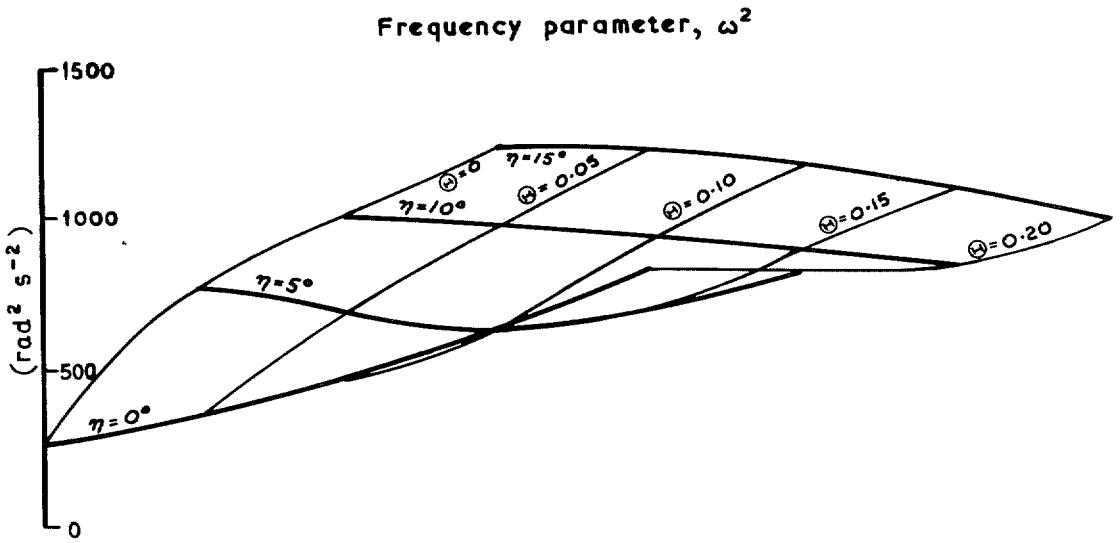

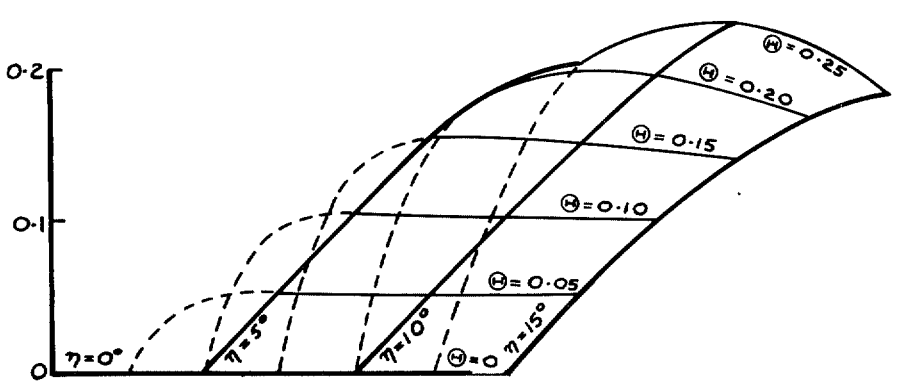

FIG. 20—continued.

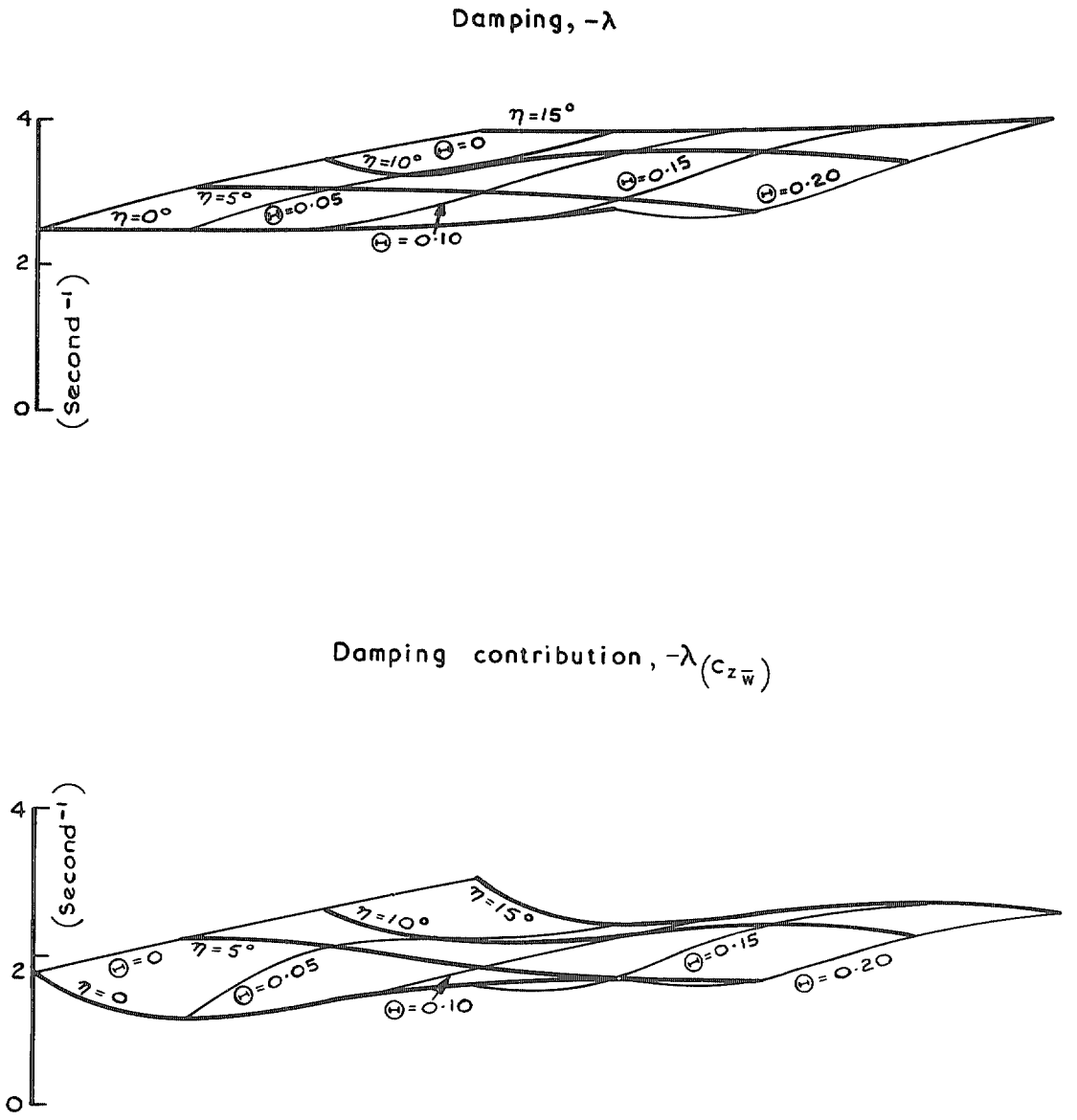

FIG. 21. Configuration 6—dynamic characteristics for $M = 2{\cdot}0$.

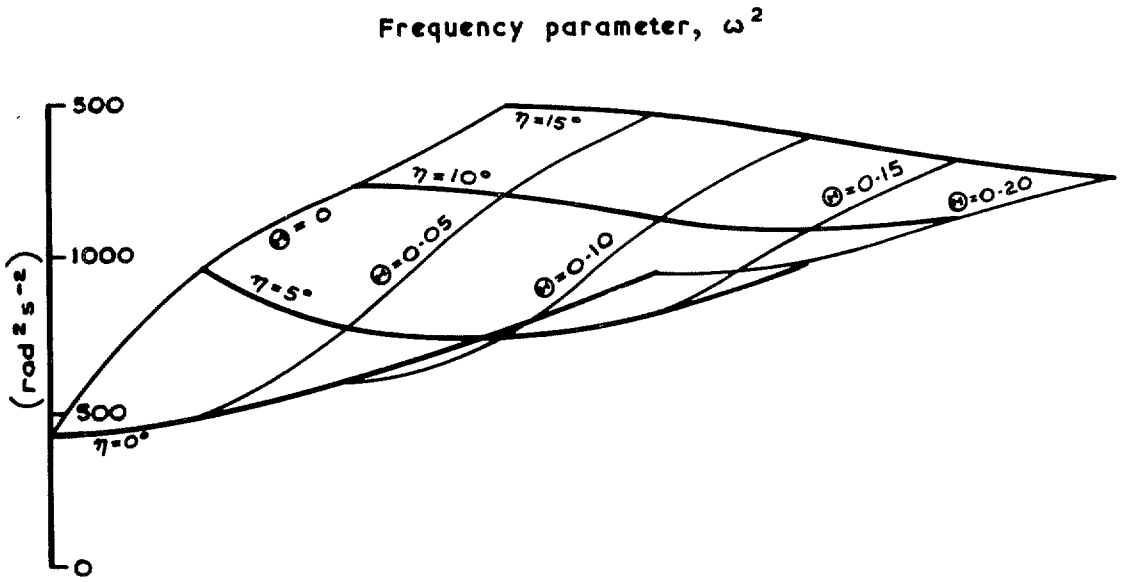

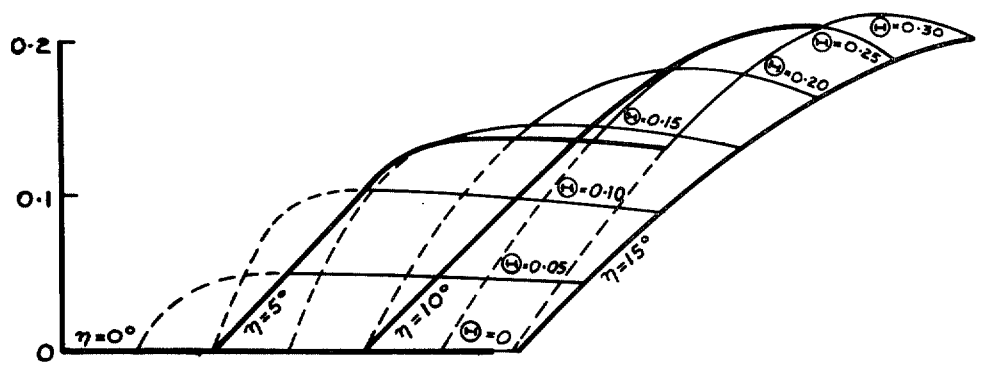

FIG. 21—continued.

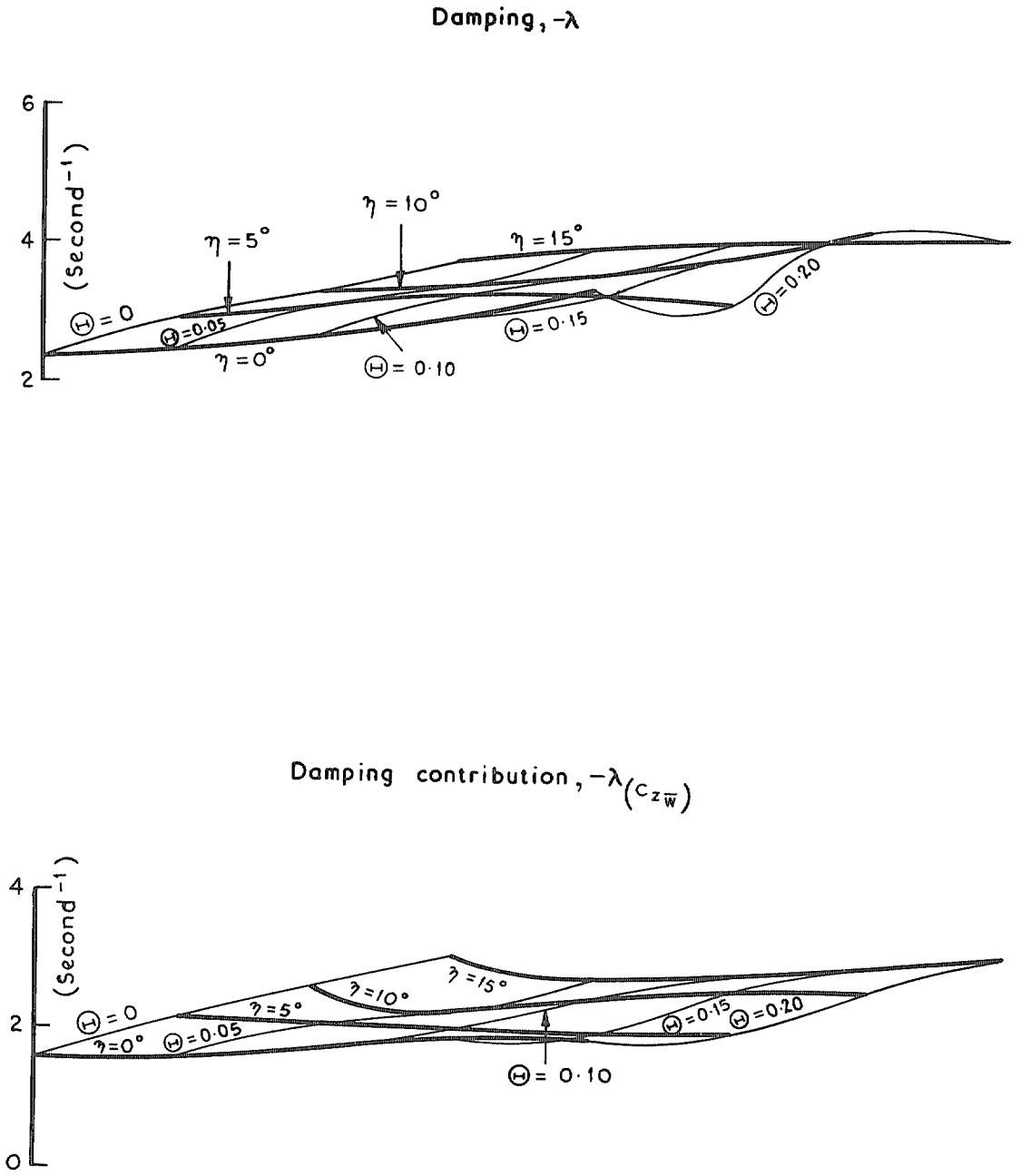

FIG. 22. Configuration 7—dynamic characteristics for $M = 1{\cdot}6$.

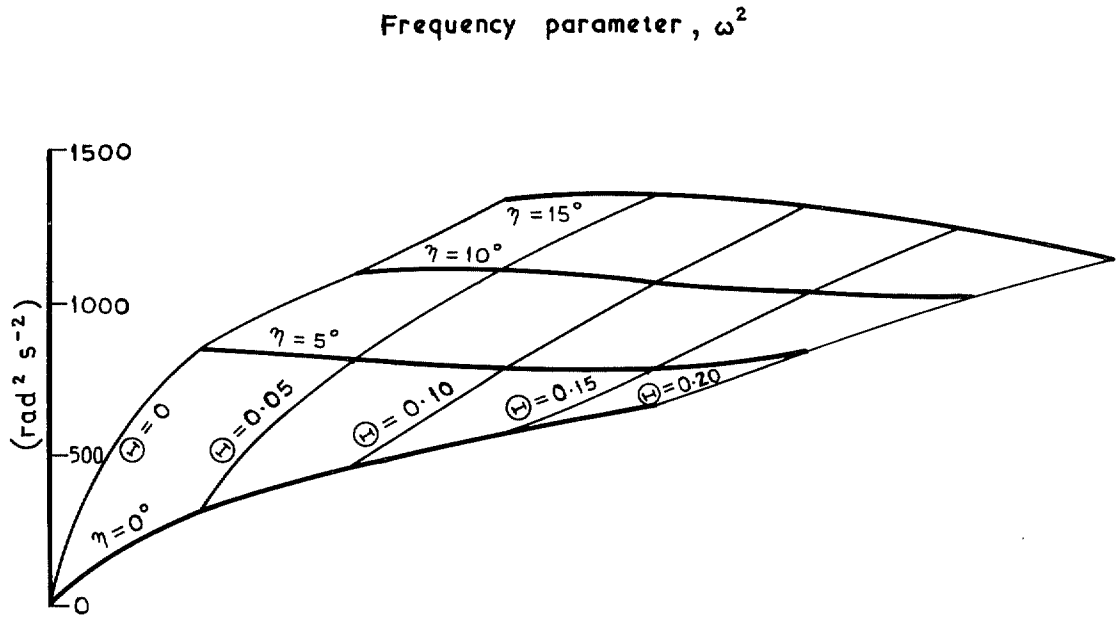

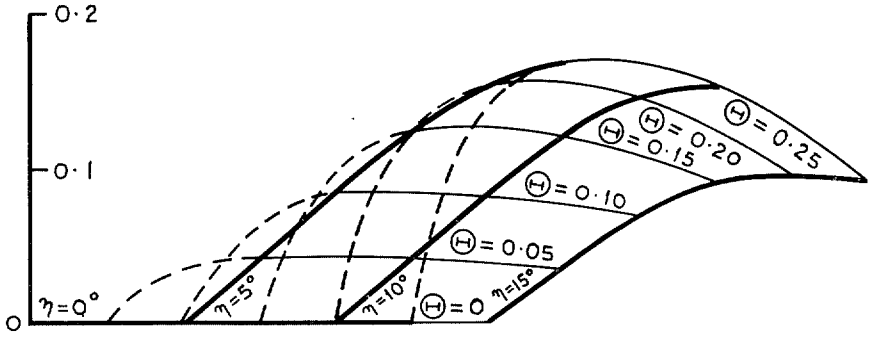

FIG. 22—continued.

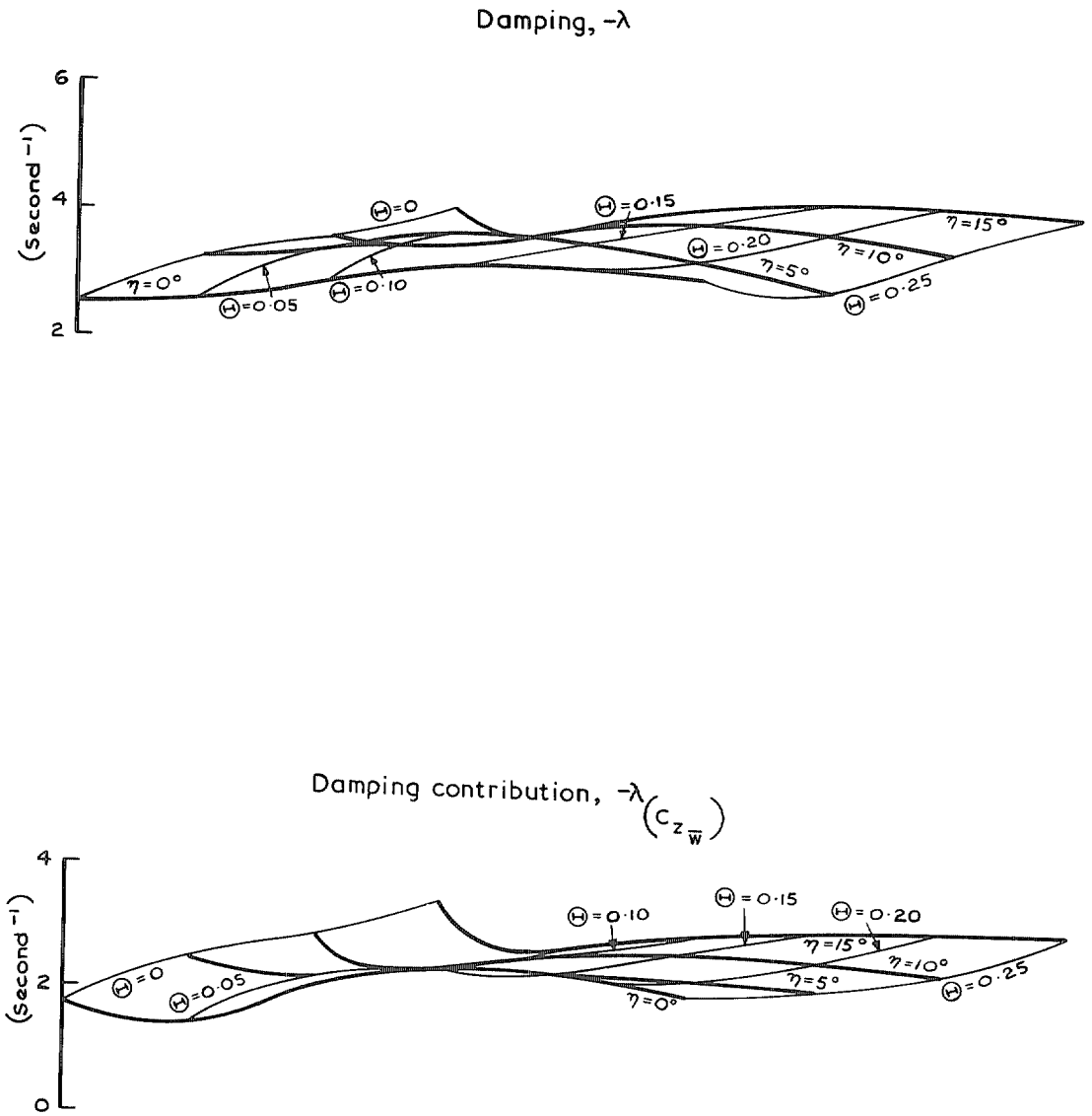

FIG. 23. Configuration 7—dynamic characteristics for $M = 2{\cdot}0$.

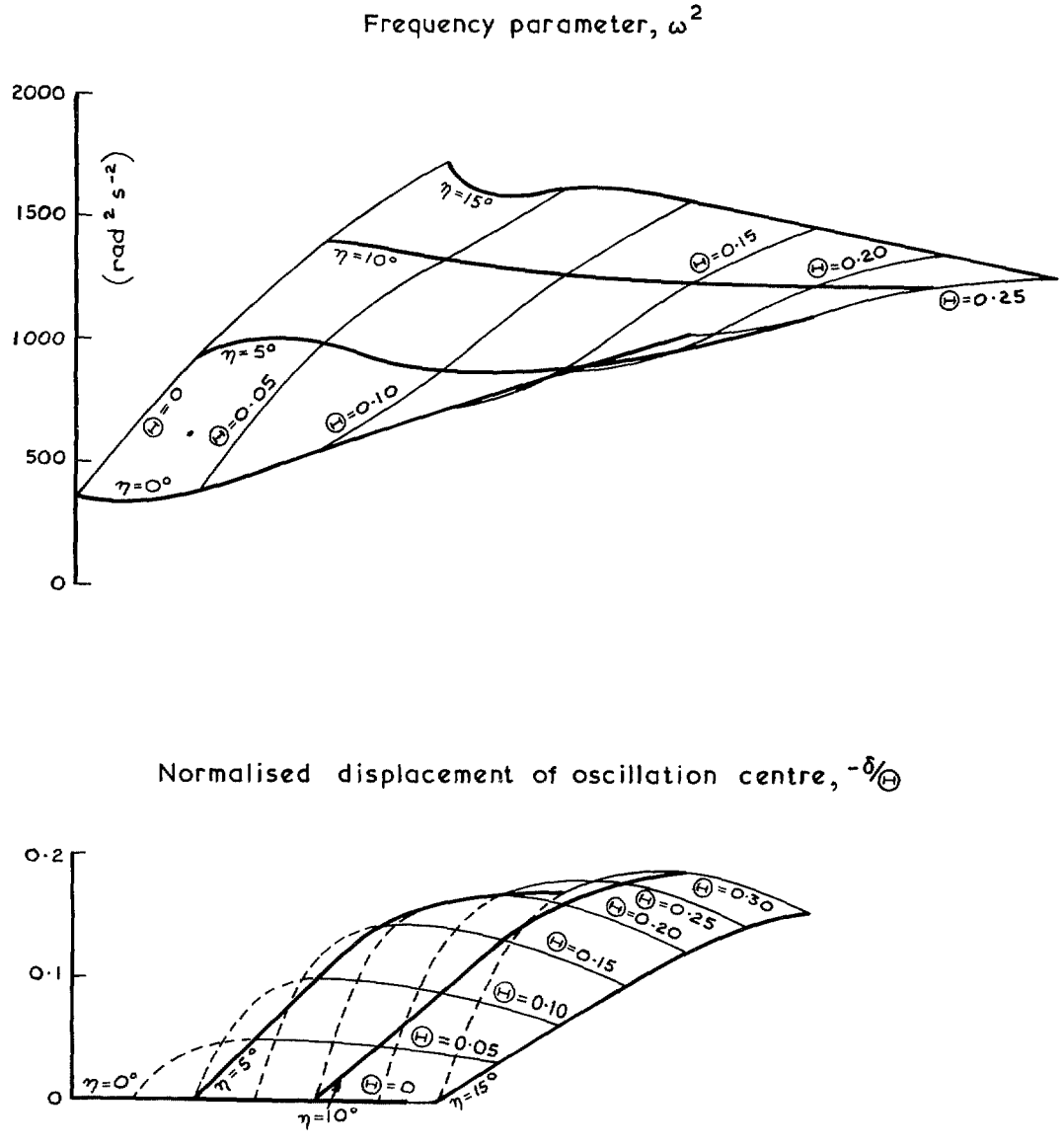

FIG. 23—continued.

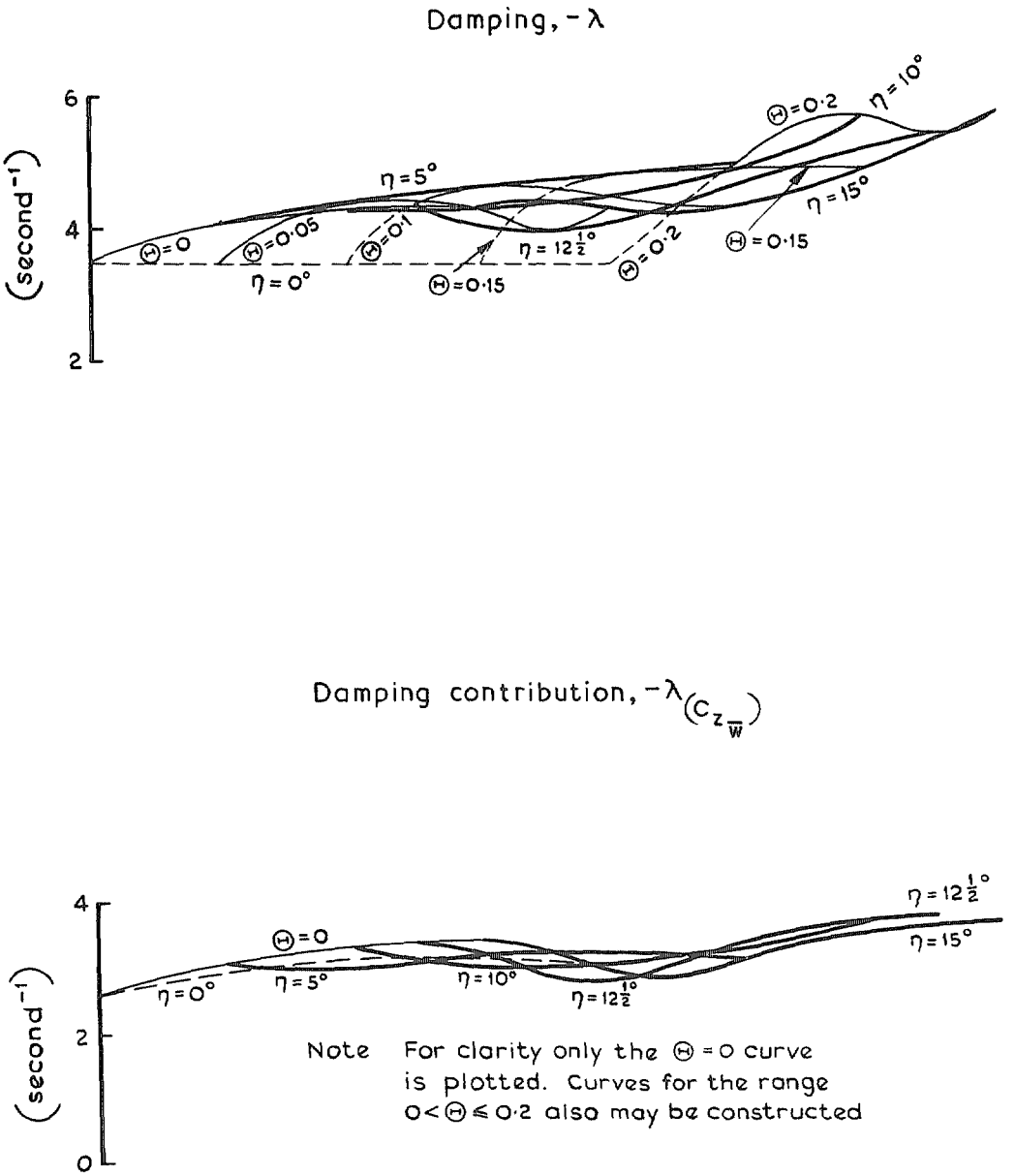

FIG. 24. Configuration 9—dynamic characteristics for $M = 1{\cdot}6$.

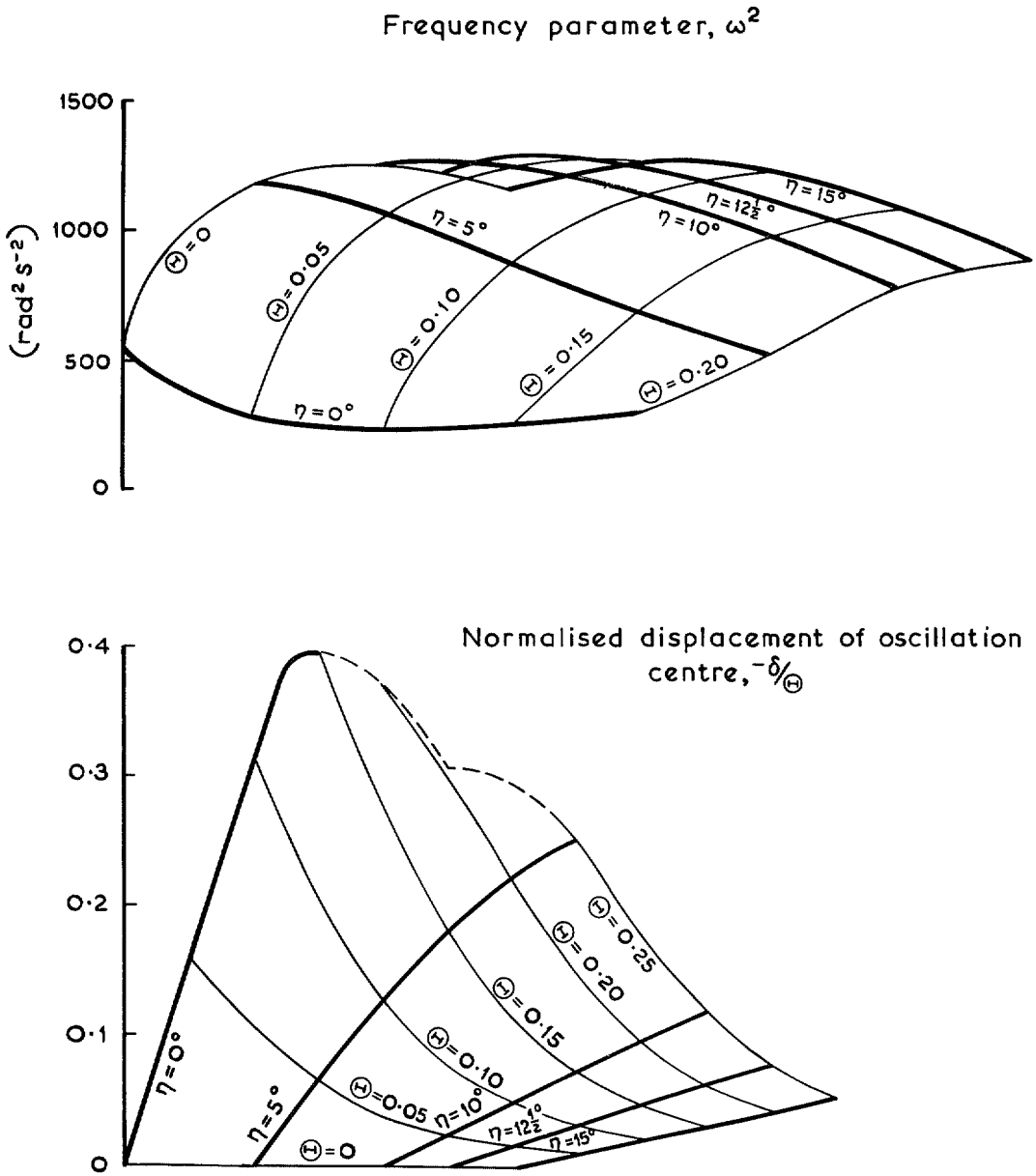

FIG. 24—continued.

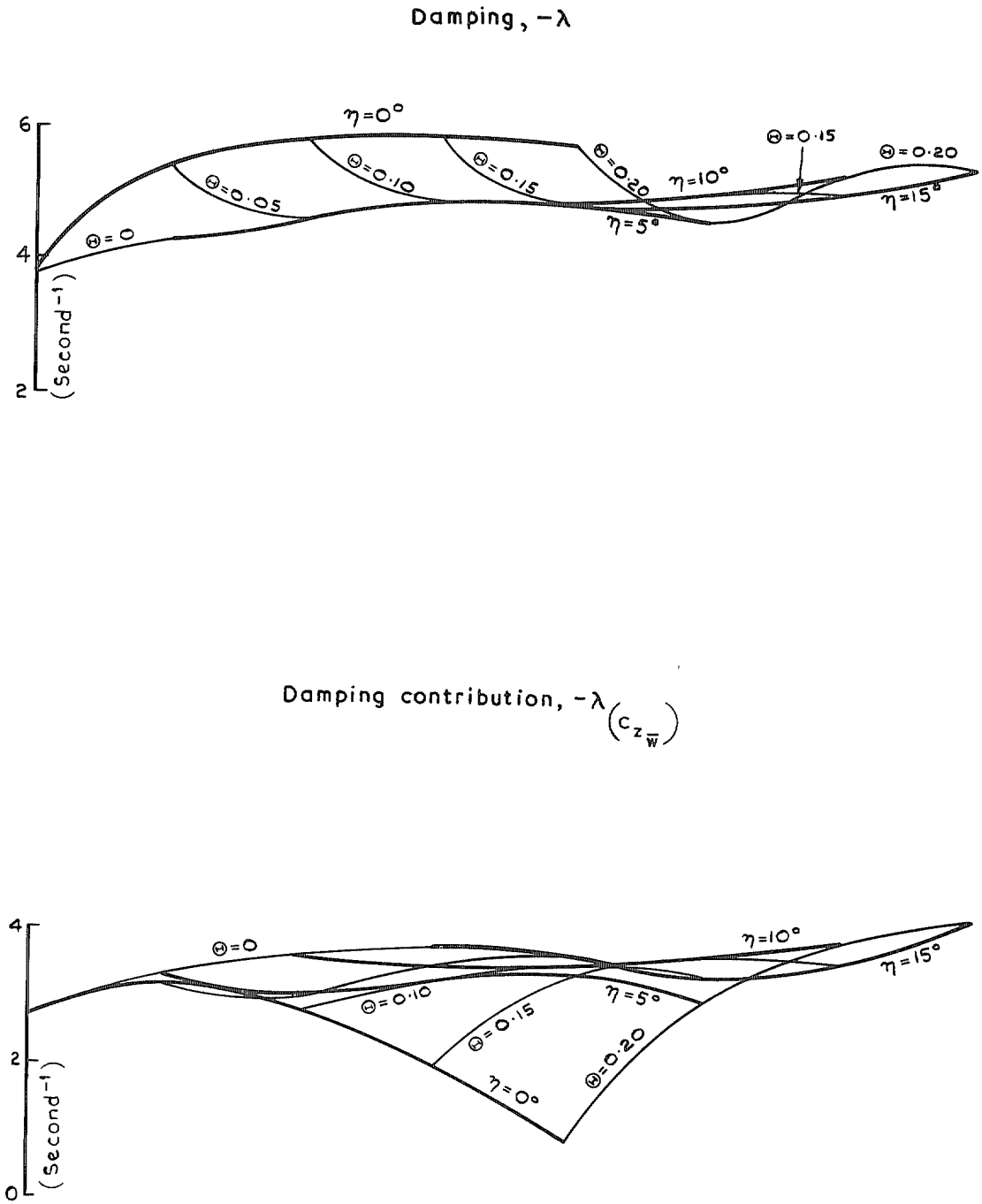

FIG. 25. Configuration 9—dynamic characteristics for $M = 2{\cdot}0$.

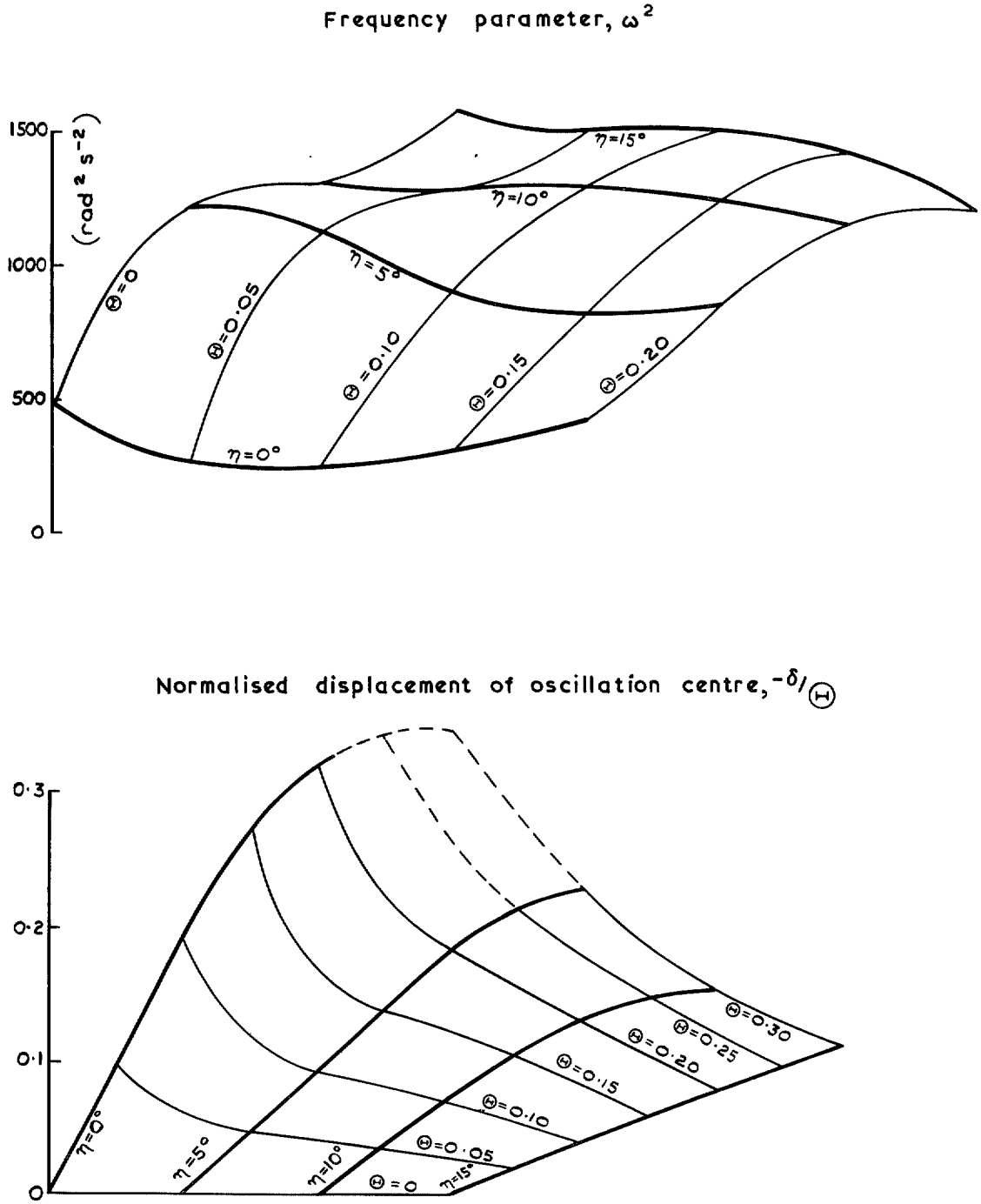

FIG. 25—continued.

Printed in England for Her Majesty's Stationery Office by J. W. Arrowsmith Ltd., Bristol BS3 2NT.
Dd. 505374 K5 3/75.

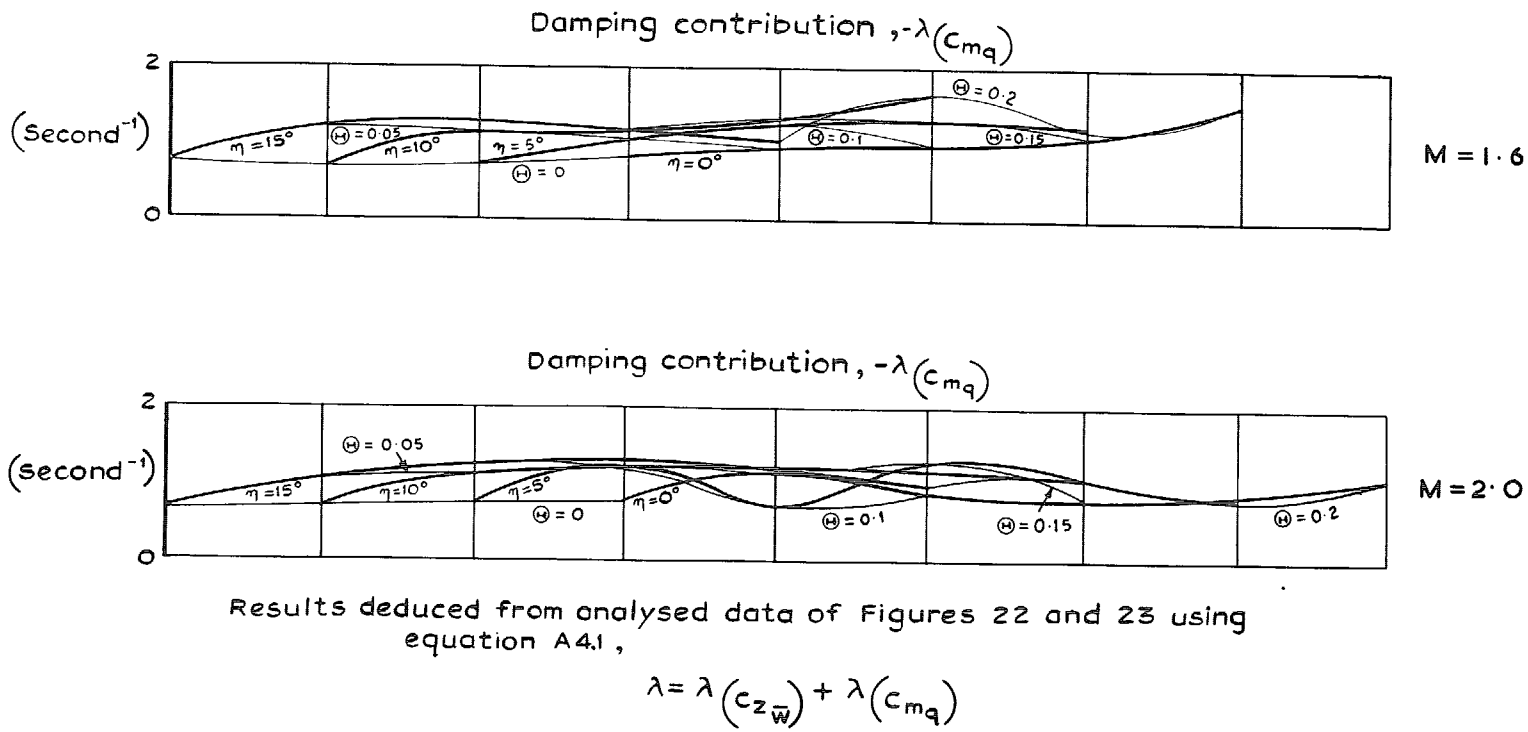

FIG. 26. Example of partitioning of damping parameter to yield damping contribution, $\lambda_{(C_{mq})}$ for configuration 7.

HER MAJESTY'S STATIONERY OFFICE

Government Bookshops

49 High Holborn, London WC1V 6HB
13a Castle Street, Edinburgh EH2 3AR
41 The Hayes, Cardiff CF1 1JW
Brazennose Street, Manchester M60 8AS
Southey House, Wine Street, Bristol BS1 2BQ
258 Broad Street, Birmingham B1 2HE
80 Chichester Street, Belfast BT1 4JY

Government publications are also available through booksellers

ISBN 0 11 470909 2